

California Department of Fish and Wildlife  
Stream Evaluation Report 2021-01

**INSTREAM FLOW EVALUATION:  
SOUTHERN CALIFORNIA STEELHEAD PASSAGE  
THROUGH THE INTERMITTENT REACH OF THE  
VENTURA RIVER, VENTURA COUNTY**

**APPENDICES**

# TABLE OF CONTENTS

Appendix A: Two-dimensional Modeling Applications, Data Sources, and Considerations .....	1
Appendix B: River 2D Pre-storm Model.....	12
Appendix C: HEC-RAS Post-storm Model .....	37
Appendix D: Pre-storm Critical Riffle Results.....	66
Appendix E: Post-storm Critical Riffle Results .....	72
Appendix F: Ventura County Survey Field Notes for Point Number 1104.....	78
References.....	82

## ABBREVIATIONS AND ACRONYMS

2D	two-dimensional (hydraulic model)
CDFW	California Department of Fish and Wildlife
cfs	cubic feet per second
cms	cubic meters per second
CMWD	Casitas Municipal Water District
CN	Courant Number
CRA	Critical Riffle Analysis
DTM	digital terrain model
DWA	diffusion wave approximation
EG	energy grade
FM	full momentum
FN	Froude number
ft	foot (feet)
GIS	Geographic Information System
GPS	Global Positioning System
HEC-RAS	Hydrologic Engineering Center's River Analysis System
LIDAR	Light Detection and Ranging
LOG	logarithm
m	meter
Net Q	net flow
PT	pressure transducer
QI	Quality Index
QL	Quality Level
RMSE	root mean square error
RTK	real-time kinematic
SZF	stage of zero flow
TIN	triangulated irregular network
USGS	United States Geological Survey
UTM	Universal Transverse Mercator
XS	cross section
WSEL	water surface elevation

# APPENDIX A: TWO-DIMENSIONAL MODELING APPLICATIONS, DATA SOURCES, AND CONSIDERATIONS

The development of a two-dimensional (2D) model generally includes these eight phases:

- 1) 2D model site selection including the limits of the upstream and downstream boundaries;
- 2) Development of a digital terrain model (DTM) for the study site;
- 3) Development of flow-water surface elevation (WSEL) relationship boundary conditions for the 2D model;
- 4) Build, best-fit computational mesh for the terrain model;
- 5) Calibrated 2D models fitting upstream discharge with downstream WSEL;
- 6) Hydraulic simulations performed at numerous flows;
- 7) Depth validation; and
- 8) Passage transect delineation.

The above phases compose the steps needed to build a 2D model and use the model to estimate depth and width for upstream migrating adult steelhead through the intermittent reach of the Ventura River. As described in Section 1.4.2 of the main report, a large storm event flooded the Ventura River Watershed in February 2017. The storm led to completion of two separate 2D models using different modeling platforms; the Pre-storm model was completed using River2D and the Post-storm model was completed using Hydrologic Engineering Center's River Analysis System (HEC-RAS). Appendix A describes the general approach of using 2D models to evaluate instream flow conditions for fish passage, site selection within the intermittent reach (Phase 1), the circumstances that led to development of two separate models, and the source and types of topographic data used to develop the pre- and post-storm DTMs (Phase 2). The data and information for Phases 3 through 8 were unique to each modeling platform. The River2D model information is provided in Appendix B and the HEC-RAS model information in Appendix C.

2D models use conservation of mass and momentum to solve for depth and velocity at each point or node for finite element models (Steffler and Blackburn 2002) or at each element or grid for finite difference models (USACE 2016). 2D model boundary conditions require that flow enter the 2D flow area through one single-thread channel at the upstream boundary, exit through a single-thread channel at the downstream

boundary, and that there are no undefined gains and losses within the 2D flow area. The 2D flow area is defined in the field by identifying the stream habitats to be assessed and then locating the required hydraulic boundaries upstream and downstream of the assessment area. 2D models require the flow-WSEL relationship defined at the upstream and downstream end of the site, with the upstream relationship used to calibrate the 2D model and the downstream relationship used as a boundary condition for the 2D model. Cross sections are established at each end of the site to measure WSEL over a range of flow targeted during study planning. Typically, field crews go out and measure discharge in or near the site, along with WSEL at the upstream and downstream boundary cross sections. The minimum number of measurements to establish a rating relationship is three (USGS 2001) while five to six is preferred.

The target flow range to evaluate fish passage in the intermittent reach was initially assumed to be between 10 to 3,000 cubic feet per second (cfs). Measuring flow and WSEL above approximately 50 cfs proved very difficult and dangerous. Timing data collection was problematic, as big storm events generating target flows in the river pass through very quickly or at night, sometimes within several hours. Though the target range was 10 to 1,000 cfs, measuring discharge and WSEL was limited to lower flows around 50 cfs and below.

## **A.1 Pre- and Post-storm 2D Models**

The study plan was to estimate depth for fish passage at potential passage barriers over a range of flows using 2D modeling techniques. The 2D model River2D (Steffler and Blackburn 2002) was chosen; the modeling platform was used previously to evaluate fish passage conditions on the Big Sur River (Holmes et al. 2016), and Butte and Mill Creeks in the Central Valley (CDFW 2018; Cowan et al. 2016). Data collection for the River2D model started in October of 2016 with three week-long trips in October, December, and January 2017 (Figure A-1). Data collection was near completion when, as discussed in the Hydrology section, a large storm flow event occurred in February 2017 (Figure A-1). Flows peaked at 18,500 cfs and the riverbed was rearranged and realigned within the study site. Fortunately, collection of the topographic survey points used to develop the DTM of the riverbed had been completed prior to the storm. The magnitude of the storm flow mobilized alluvial deposits that buried several pressure transducers (PTs) recording water level along the model boundary cross sections. Staff were able to recover the PTs placed along the downstream boundary cross sections (XS-1) and one of the PTs along the upstream boundary cross section (XS-2); refer to Figure 11 in the main report.

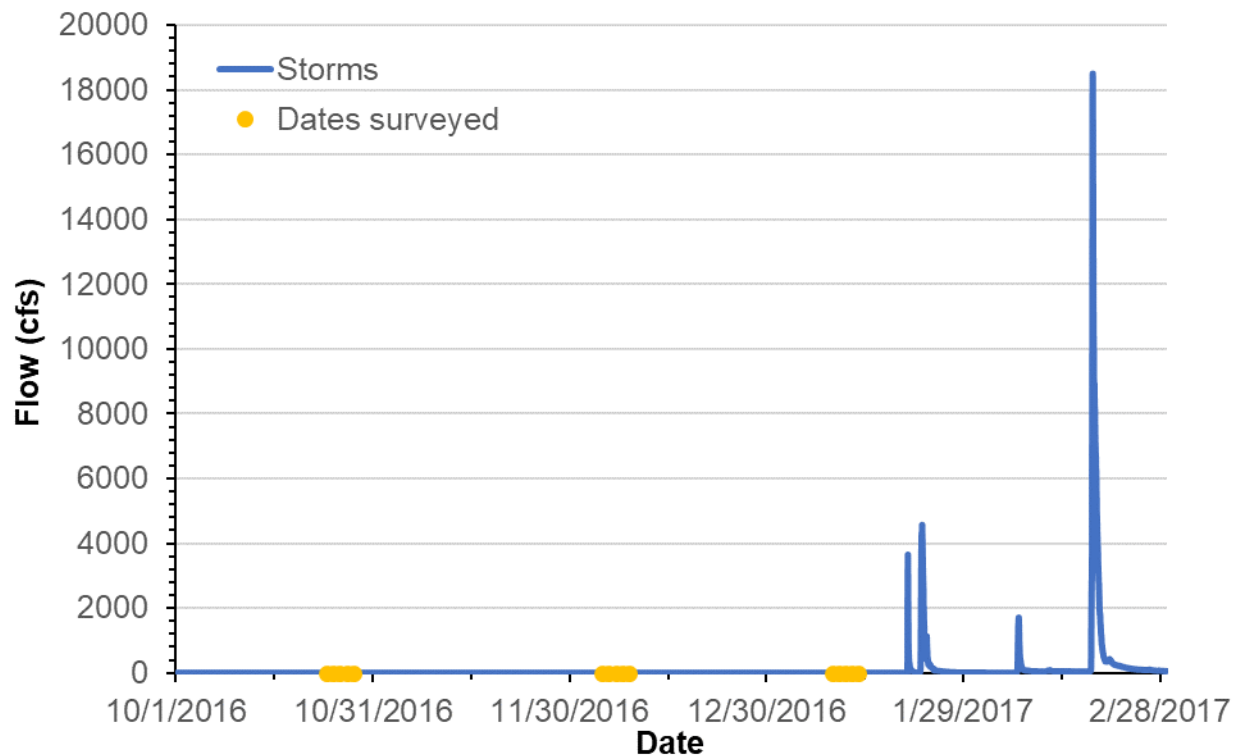


**Figure A-1.** Hydrograph of storm events from 15-minute data provided by USGS gage 11118500, located near Foster Park (in blue), and three separate week-long topographic survey events to develop the digital terrain for the 2D model (yellow segments).

Prior to the storm, staff were not able to survey the study site for potential impediments to fish passage that typically occur at flow-sensitive riffles because the study site was dry. Staff had also not yet collected validation data consisting of random water depth measurements within the 2D flow area. The absence of the critical riffle survey was overcome using the model results for water depth. Staff searched the model simulations to detect shallow, passage-limiting areas near the sites evaluated by the Casitas Water District study (Lewis and Gibson 2009) and the critical riffles surveyed post-storm by staff in April 2017. The River2D model is referred to here as the Pre-storm model.

After the occurrence of the February 2017 storm, CDFW decided to prepare a second 2D model to evaluate the study area post-storm to detect whether the movement of the streambed substrates during a channel forming flow event would change the amount of water needed for fish passage. Data collection started in April 2017 when the critical riffle survey was completed. The topographic survey data were collected during four separate trips that started in November 2017 and finished in June 2018 (Figure A-2). Over the period the surveying was performed two storms occurred within that timeframe with peak flows as follows: 6,120 cfs on January 9, 2018 and 4,650 cfs on March 22, 2018.

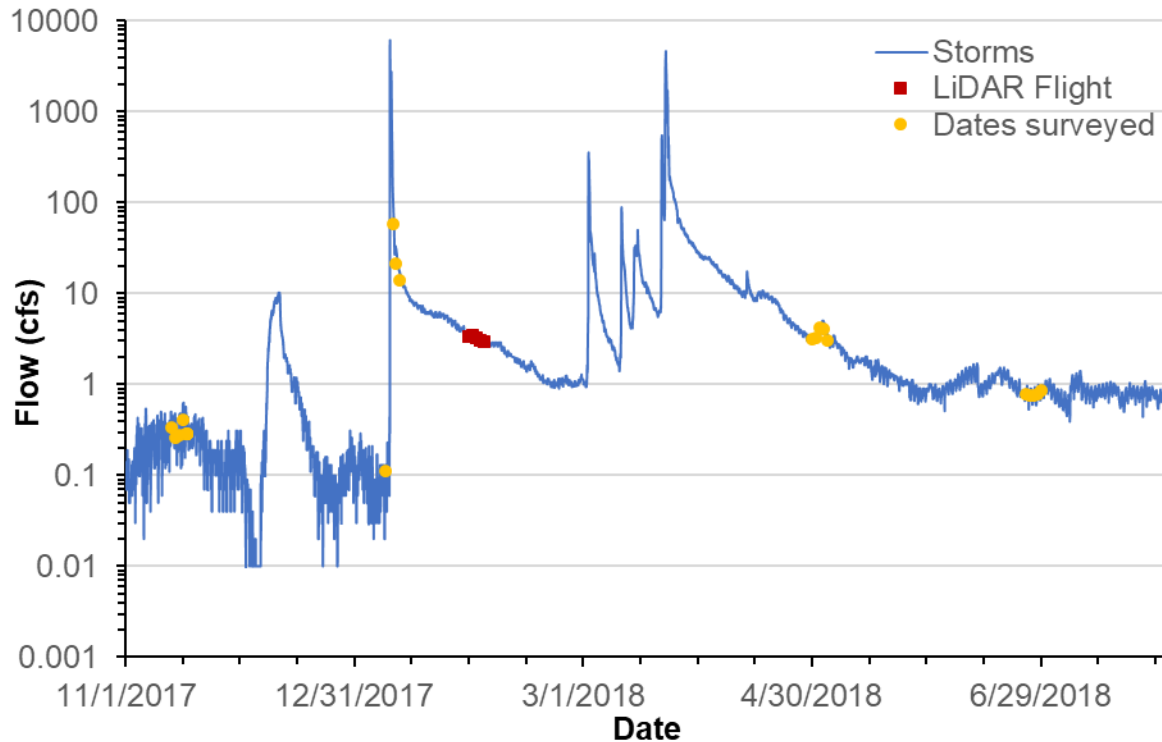


**Figure A-2.** Log-scale hydrograph of storm events from 15-minute data provided by USGS gage 11118500 located near Foster Park (in blue), the four weeks when CDFW staff surveyed the river channel to develop the digital terrain for the 2D model (yellow segments), and the timing of the Light Detection and Ranging (LIDAR) flight (red segment).

HEC-RAS version 5.0.7 (HEC-RAS 2018) was selected to predict depth and width for fish passage within the study site post-storm. The most recent version of HEC-RAS has improved GIS functionality in its RAS-Mapper utility. DTMs in HEC-RAS are raster-based. Raster files can be layered on top of one another together when generating the DTM in HEC-RAS. This feature was important for the Post-storm model because the Post-storm DTM was completed using a combination of rasters generated from topographic points collected in the field after the storm and high resolution, 0.25-meter (m) LIDAR data, flown after the storm. The descending limb of the storm prior to the high-resolution LIDAR flight was used to calibrate the HEC-RAS model.

## A.2 Digital Terrain Model using LIDAR

LIDAR technology was used to supplement the topographic survey data in both 2D models. LIDAR is collected using airplane mounted equipment. Flights are performed over the desired area and produce a point-grid interpretation of the land surface flow. Two sets of LIDAR data are available through the Ventura County Watershed Protection District web portal. The first LIDAR set was flown by Airborne 1 and published for the

county on September 26, 2005 (Airborne 1 2005). The resolution of the point grid was 3 m or approximately 10 feet (ft). The 2005 LIDAR data were used to fill in areas outside the main channel to allow higher flows (up to 3,000 cfs) to be simulated. Those areas included over-bank zones, floodplains, intermittent side channels, areas consumed by *Arundo donax*, and private property within the floodplain.

The second set of LIDAR available through the County web portal is from 2018 (Towill Inc 2018). The flight was flown by Airborne LIDAR Data from January 30, 2018 through February 3, 2018 in response to the Thomas Fire and Montecito Debris Flows. The accuracy of a LIDAR flight is described by the USGS as quality levels (QL) 0-3, with quality level 0 (QL0) being the highest having a root mean square error (RMSE) in the z direction of 5.0 cm or less, QL1 and QL2 having a RMSE of 10.0 cm with QL1 having a higher pulse density, and QL3 with RMSE of 20.0 cm or less (USGS 2018). The 2018 Ventura County flight was performed at QL1 accuracy with a grid point density of 0.25 m. Converting the 10.0 cm to ft, the 2018 QL1 level LIDAR data had a standard RMSE in the z-direction of approximately 0.3 ft. The LIDAR flight metadata reported that 50 check points were recorded via Global Positioning System (GPS) ties to the 8 CORS/PBO (Continuously Operating Reference Stations and Plate Boundary Observatory) station network used for the primary survey network (Towill Inc 2018). The data verification consisted of 32 non-vegetated check points and 18 vegetated check points. The non-vegetated vertical accuracy analysis statistics were as follows: the RMSE in the z-direction of the 36 non-vegetated points was 0.034 m (0.11 ft), with an average error of -0.005 m, and a standard deviation of 0.034 m. Thus, the 2018 LIDAR data had a vertical accuracy of 0.11 ft, versus 0.1 ft for the survey data. Almost all the portion of the site inundated at flows up to 300 cfs was non-vegetated.

Timing of the 2018 LIDAR flight was less than two months after the storm events that were used to develop the Post-storm WSEL/flow rating relationship. The timing of the 2018 LIDAR flight ensured the stream channel structure would not have changed after the flows used to calibrate the model. The 2018 flight resolution was so fine that large portions of the site were modeled using the 0.25-m LIDAR data. The 2018 LIDAR data were augmented with the Post-storm topographic field survey data in those areas with pooled water.

### **A.3 Survey Control**

In order to use the 2018 LIDAR topographic data in conjunction with the topographic data and water level collected by staff in the field, the horizontal and vertical survey controls had to be verified and adjusted accordingly to allow the two data sets to be used together. A total of 26,407 points were collected using the Real-time kinematic (RTK) GPS and the total station; 5 points were deleted because they were duplicates of existing points, and 23 points were deleted because there had erroneous elevations that

could not be corrected. In total, 26,379 topographic survey points were used to create the survey based DTM. The survey points were compared with the 2018 LIDAR by extracting the elevations from the LIDAR digital elevation model at each survey point. The LIDAR digital elevation model was found to have a consistent positive vertical offset of approximately 0.238 m compared to the field survey points (Table A-1). The vertical offset was added to the elevations of each topographic survey point used the model including PT and WSEL data. In 2020, after staff were authorized to return to the field, a series of five static surveys were performed to reestablish vertical control at the study site and confirm that the coordinate plane of the topographic survey data collected by staff and the LIDAR data were parallel.

**Table A-1.** Comparison of elevation data between the 2018 LIDAR and topographic survey data collected by staff using real-time kinematic (RTK) GPS and total station.

<b>Statistic</b>	<b>Elevation Difference from LIDAR vs. RTK GPS and Total Station (m)</b>
Maximum	3.224
Minimum	-2.043
Standard Deviation	0.261
Average	0.260
Median	0.238

Site surveys were conducted using a Universal Transverse Mercator (UTM) projection in metric units. The study site was located in Zone 11; the horizontal datum was NAD83(2011), Epoch 2010.0, and the vertical datum was NAVD88. Survey control for both the Pre-storm and Post-storm models was initially established in October 2016 by reoccupying an existing benchmark located on the east side of the bridge that crosses over the Ventura River at Santa Ana Boulevard, referred to here as Base1 (Figure A-3). The benchmark was in a flat area just south of the guardrail (Figure A-4)<sup>a</sup>.

<sup>a</sup> <https://www.ngs.noaa.gov/OPUS/getDdatasheet.jsp?PID=BBGY43&ts=20267130257>

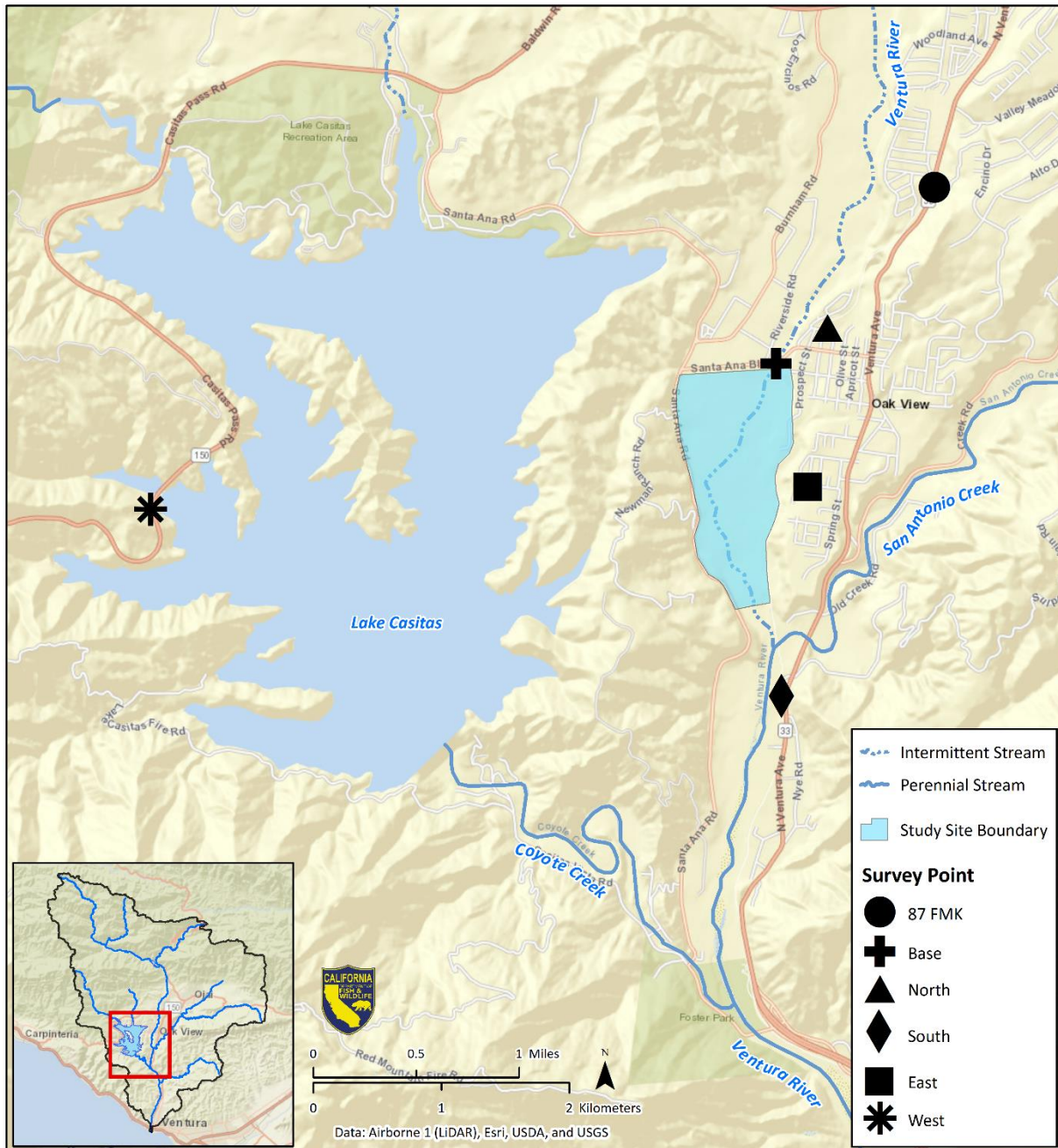


Figure A-3. Static survey area map.



**Figure A-4.** Survey benchmark located southeast of Santa Ana Boulevard bridge.

Vertical control for the study was originally established by locating a known point in the area using the National Geodetic Survey Data Explorer (NOAA 2020a). A point was found near the study site, “87 FMK” (Figure A-3). This was a vertical control only point, where a RTK rover on a two m pole was set over 87 FMK, leveled with a bipod, and run in autonomous mode for approximately 20 minutes to establish horizontal coordinates (Table A-2). The newly established horizontal coordinates and existing vertical elevation were used to set the RTK base unit over 87 FMK. The rover unit was set up at Base1 in the same fashion as at 87 FMK and was run in Fixed Only mode, collecting global positioning data using fixed point precision settings of 0.03 m in the horizontal and 0.015 m in vertical. The RTK rover was run for 600 counts to generate horizontal and vertical coordinates at Base1 (Table A-2).

**Table A-2.** Survey control point coordinates.

Point	Northing (m)	Easting (m)	Elevation (m)
87 FMK	3810257.96	289098.35	182.840
Base1 (10/26/2016)	3808880.21	287861.12	125.592
Base1 plus 0.238-m offset	3808880.21	287861.12	125.830
Point 1104 (1/29/2020)	3808879.85	287860.32	125.838
Static Survey (9/16/2020)	3808880.01	287860.16	125.841

The point Base1 was originally installed and established by Ventura County. The Ventura County Surveyor's Office kindly provided the field notes for the benchmark, referred to by Ventura County (County) as point number 1104. The County's field notes are provided in Appendix F. The County's most recent visit to point 1104 was on January 29, 2020. A position for point 1104 was generated in State Plane Coordinates, Zone 5, 2004 Epoch (US Ft). The National Geodetic Survey *Online Vertical Datum Transformation* tool (NOAA 2020b) was used to convert the coordinates into the project UTM projection. The County derived elevation for point 1104 was within 0.008 m of the assumed offset elevation (Table A-2).

On September 16, 2020, static surveys were performed at five locations, the study benchmark Base1, and four other points that bounded the study site and that were within the boundary of the 2018 LIDAR (Figure A-3). The static survey locations were chosen based on their relative position in reference to the study site (north, south, east, west), flat areas where the LIDAR elevation was expected to be consistent across the 0.25-m grid, and locations where it would be safe to set up the equipment to run for more than four hours. Digital images of the static survey locations are provided in Figure A-4 for Base1 and Figure A-5 for the north, south, east, and west points.



**Figure A-5.** Static survey locations north, south, east, and west from left to right and top to bottom.

The output files from the static surveys were uploaded to the Online Positioning User Service (NOAA 2020c) to generate a coordinate solution for each point. The resulting coordinates from the solution for Base1 are given in Table A-2. The static survey elevation of Base1 was within 0.003 m of the County’s transformed elevation. The static survey point coordinates for all five points were loaded into ArcGIS and elevations were extracted from the 2018 LIDAR at each point. The results of the point elevation extractions are provided in Table A-3.

**Table A-3.** Static survey results.

<b>Point</b>	<b>Northing (m)</b>	<b>Easting (m)</b>	<b>Static Survey Elevation (m)</b>	<b>LIDAR Elevation (m)</b>	<b>Difference (m)</b>	<b>Duration of Static Survey (hours)</b>
Base1	3808880.01	287860.16	125.841	125.790	0.054	5.5
North	3809159.26	288260.45	148.654	148.590	0.064	4.3
South	3806280.47	287902.02	93.417	93.350	0.067	5.3
East	3807915.83	288105.94	157.959	157.900	0.059	5.5
West	3807740.35	282969.04	186.233	186.230	0.003	4.0

The static survey results indicated that the LIDAR elevations were slightly lower than the static survey elevations of the points located within the general drainage area of the intermittent reach (points Base1, North, South, and East). The static survey point West was the highest point and had equal elevation to the LIDAR data. No tilt was detected between the LIDAR surface and the static survey points collected nearest the study site, excluding the West point. The average difference between the nearest static survey points and the elevations extracted from the LIDAR was consistently 0.06 m. This was comparable to the accuracy of the static survey elevations (ranging from 0.054 m to 0.06 m). The West point elevation was the farthest from Base1 and was also the highest elevation point.

The purpose of this evaluation was to determine whether the vertical offset previously applied to the topographic survey data collected using RTKs and Total Station should be adjusted or maintained. The original offset of 0.238 m was based on the median difference in elevation between the 26,379 Post-storm model survey points and the corresponding elevations extracted from the 2018 LIDAR. The original offset was added to the initial Base1 elevation of 125.592 m, resulting in an adjusted vertical control elevation of 125.830 m. The static survey performed at Base1 produced a vertical control elevation of 125.841 m. The elevation at Base1 extracted from the 2018 LIDAR was 125.790 m. The 2018 LIDAR elevation may be impacted by the rough ground conditions at the site of Base1 and the benchmark being slightly elevated above the ground level (Figure A-4). The original vertical offset of 0.238 m was increased to 0.249 m based on the result of the static survey at Base1. The static survey data confirmed the accuracy of the LIDAR data elevations, given that the difference in elevations between the static survey and LIDAR are comparable to the accuracy of the static survey elevations.

## **APPENDIX B: RIVER 2D PRE-STORM MODEL**

This Appendix presents the River2D model calibration methods and results for the Pre-storm two-dimensional model created to evaluate passage conditions for upstream migration of adult steelhead through the intermittent reach of the Ventura River. This section presents the results of the WSEL calibration at the model boundary cross sections, the calibration of simulated versus measured hydraulic data within each model simulation, and hydraulic parameter settings used to achieve convergence of the model simulation results with the hydraulic data measured in the field.

### **B.1 WSEL Calibration Methods**

The desired flow range to evaluate fish passage in the intermittent reach was initially assumed to be between 10 to 3,000 cfs. The initial flow range was based upon the results of the 2010 Robles Fish Passage Facility Progress Report (CMWD 2010). Measuring WSEL and flow directly in the field proved very difficult. Timing data collection was problematic, as big storm events generating target flows in the river pass through very quickly or at night, sometimes within several hours. Discharge in the study site was estimated by assuming the flow entering the site was equal to the flow recorded at Foster Park minus the flow contribution from San Antonio Creek (Figure B-1). The water levels recorded by the PTs at XS-1 and XS-2 were paired with the flows reported at Foster Park factored to represent the study site flow.

The relationship between flow at Foster Park and water level in the site is dependent upon the time required for water to travel through the site and arrive at Foster Park. Travel time is a function of travel distance and the average water velocity, where average velocity is proportional to flow magnitude. Travel time was estimated by reviewing the data from Foster Park over the period when the PTs were in place. The water stage data from Foster Park was compared with the water level data from the PTs (Figure B-1) to identify unique peaks and valleys common to each dataset but offset in time.

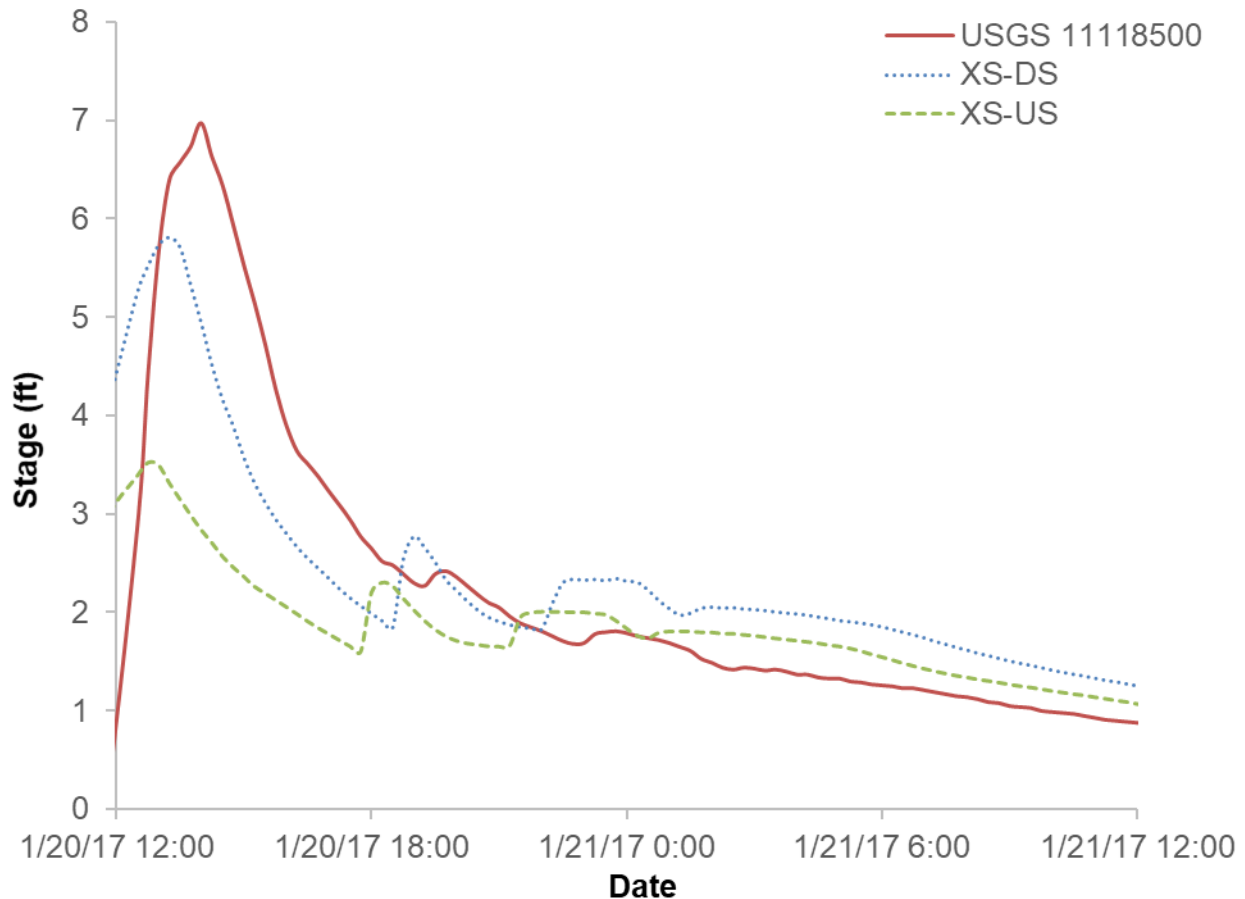


**Figure B-1.** Timing of water stage recorded at Foster Park versus water level measured by the PTs located in the Pre-storm 2D flow area boundary cross sections. Data in figure spans 1/20/2017 12:00 PM to 1/21/2017 12:00 PM.

Once the travel times were defined, the stage data could be shifted in time and rating relationships could be developed for each boundary cross section. The hydrograph from the Foster Park gage was reviewed to identify receding limbs following storm events. The 15-minute discharge data from those receding limbs were plotted with the water level data from each boundary cross section. The water levels were converted to WSEL from benchmark survey data. Logarithmic regression equations were used to develop predictive rating relationships for flow and WSEL. The downstream hydraulic control point for each boundary cross section was identified and surveyed. The downstream hydraulic control point, referred to here as the stage of zero flow (SZF), was subtracted from each WSEL used in the regression. The ratings were developed by plotting the logarithm (LOG) of 15-minute discharge versus the LOG of the WSEL minus the SZF. By plotting the data on LOG-LOG scale, a linear best-fit relationship is produced. The linear best-fit equation is then used to predict WSEL over a range of flows. This overall technique employing the SZF and logarithmic scales is referred to here as LOG-LOG regression.

## B.2 River2D Model Construction Methods

The total station, RTK GPS, and LIDAR data were combined in a spreadsheet to create the input bed file for River2D. The bed files contain the horizontal location (northing and easting), bed elevation, and initial bed roughness value for each point. The initial bed roughness value for each point was determined from the substrate and cover codes for that point and the corresponding bed roughness values in Table B-1, with the bed roughness value for each point computed as the sum of the substrate bed roughness value and the cover bed roughness value for the point. Substrate and cover codes were assigned to the LIDAR data in ArcGIS using Theissen polygons derived from the total station and RTK GPS points. The resulting initial bed roughness value for each point was therefore a combined matrix of the substrate and cover roughness values. The bed roughness values for substrate in Table B-2 were computed as five times the average particle size<sup>b</sup>. The bed roughness height values for cover in Table B-3 were computed as five times the average cover size, where the cover size was measured on the Ventura River on a representative sample of cover elements of each cover type. The bed files were exported from the spreadsheet as ASCII files.

**Table B-1.** Substrate codes, descriptors and particle sizes used for Ventura River 2D models.

Code	Type	Particle Size (inches)
0.1	Sand/Silt	< 0.1
1	Small Gravel	0.1 – 1
1.2	Medium Gravel	1 – 2
1.3	Medium/Large Gravel	1 – 3
2.3	Large Gravel	2 – 3
2.4	Gravel/Cobble	2 – 4
3.4	Small Cobble	3 – 4
3.5	Small Cobble	3 – 5
4.6	Medium Cobble	4 – 6
6.8	Large Cobble	6 – 8
8	Large Cobble	8 – 10
9	Boulder/Bedrock	> 12
10	Large Cobble	10 – 12

<sup>b</sup> Five times the average particle size is approximately the same as two to three times the D85 particle size distribution metric, which is recommended as an estimate of bed roughness height Yalin (1977).

**Table B-2.** Cover coding system used for Ventura River 2D models.

<b>Cover Category</b>	<b>Cover Code</b>
No cover	0
Cobble	1
Boulder	2
Fine woody vegetation ( $\leq 1''$ diameter)	3
Fine woody vegetation + overhead	3.7
Branches	4
Branches + overhead	4.7
Log ( $> 1'$ diameter)	5
Log + overhead	5.7
Overhead cover ( $> 2'$ above substrate)	7
Undercut bank	8
Aquatic vegetation	9
Aquatic vegetation + overhead	9.7
Rip-rap	10

**Table B-3.** Initial bed roughness height values used for Ventura River River2D models.

<b>Substrate Code</b>	<b>Substrate Bed Roughness (m)</b>	<b>Cover Code</b>	<b>Cover Bed Roughness (m)</b>
0.1	0.05	0.1	0
1	0.1	1	0
1.2	0.2	2	0
1.3	0.25	3	0.11
2.3	0.3	3.7	0.2
2.4	0.4	4	0.62
3.4	0.45	4.7	0.96
3.5	0.5	5	1.93
4.6	0.65	5.7	2.59
6.8	0.9	7	0.28
8	1.25	8	2.97
9 <sup>c</sup>	0.05, 0.76, 2	9	0.29
10	1.4	9.7	0.57
N/A	N/A	10	3.05

<sup>c</sup> For substrate code 9, we used bed roughness of 0.76 and 2, respectively, for cover codes 1 and 2, and a bed roughness of 0.05 for all other cover codes.

A pre-processor utility program, R2D\_BED (Steffler 2002), is used to develop the DTM of the study area. Additional topography data were collected to develop an extension one channel-width long upstream of the study site, to enable the flow to be distributed by the model when it reached the study area. This extension minimized boundary conditions influencing the flow distribution at the upstream boundary cross section and within the study site. R2D\_BED was used to define the study area boundary and to refine the raw topographical data triangulated irregular network (TIN) by defining breaklines<sup>d</sup> following longitudinal features such as thalwegs, tops of bars, and bottoms of banks. The first step in refining the TIN was to conduct a quality assurance/quality control process, consisting of a point-by-point inspection to eliminate quantitatively wrong points, and a qualitative process where we checked the features constructed in the TIN against aerial photographs and site photographs to make sure we had represented landforms correctly. Breaklines were also added along lines of constant elevation.

An additional utility program, R2D\_MESH (Waddle and Steffler 2002), was used to define the inflow and outflow boundaries and create the finite element computational mesh for the River2D model. R2D\_MESH uses the final bed file as an input. The first stage in creating the computational mesh was to define mesh breaklines<sup>e</sup> which coincided with the final bed file breaklines. Additional mesh breaklines were then added between the initial mesh breaklines, and then additional nodes were added as needed to improve the fit between the mesh and the final bed file and to improve the quality of the mesh, as measured by the Quality Index (QI) value. An ideal mesh (all equilateral triangles) would have a QI of 1.0. A QI value of at least 0.2 is considered acceptable (Waddle and Steffler 2002). The QI is a measure of how much the least equilateral mesh element deviates from an equilateral triangle. The final step with the R2D\_MESH software was to generate the computational mesh (.cdg file format). The process of creating the DTM in River2D is explained graphically in Figure B-2.

---

<sup>d</sup> Breaklines are a feature of the R2D\_Bed program which force the TIN of the bed nodes to linearly interpolate bed elevation and bed roughness values between the nodes on each breakline and force the TIN to fall on the breaklines (Steffler 2002).

<sup>e</sup> Mesh breaklines are a feature of the R2D\_MESH program which force edges of the computation mesh elements to fall on the mesh breaklines and force the TIN of the computational mesh to linearly interpolate the bed elevation and bed roughness values of mesh nodes between the nodes at the end of each breakline segment (Waddle and Steffler 2002).

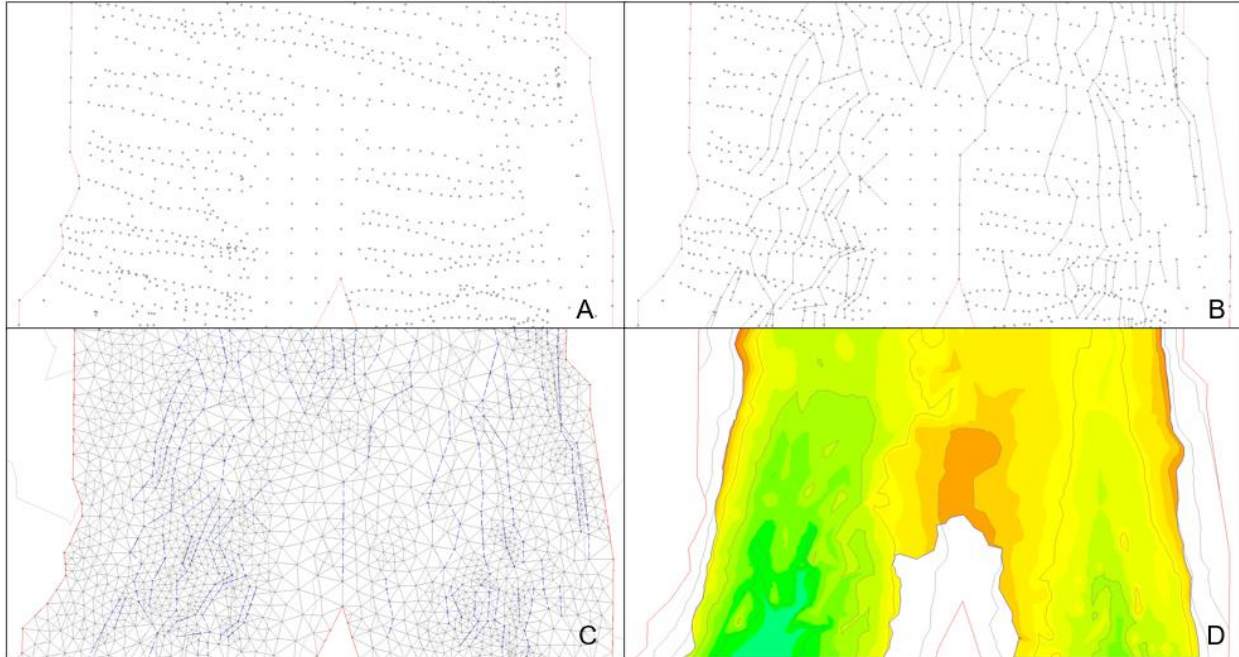


**Figure B-2.** River2D model construction stages: (A) import raw bed topography points into R2D\_BED; (B) add breaklines in R2D\_BED; (C) add computational mesh and mesh breaklines in R2D\_MESH; and (D) final DTM in River2D.

### **B.3 River2D Model Calibration Methods**

Once a River2D model has been constructed, calibration is required to determine that the model is reliably simulating the flow-WSEL relationship determined through the WSEL calibration process, using the measured WSELs. The cdg files were opened in the River2D software, where the bed topography and computational mesh were used together with the WSEL at the bottom of the site, the flow entering the site, and the bed roughness heights of the computational mesh elements to compute the depths, velocities, and WSELs throughout each site. The basis for the current form of River2D is given in Ghanem et al. (1996). The computational mesh was run to steady state at the highest flow simulated and the WSELs predicted by River2D at the upstream end of the site were compared to the WSELs predicted at the upstream boundary cross section. Calibration was considered to have been achieved when the WSELs predicted by River2D at the upstream boundary cross section were within 0.1 ft (0.031 m) of the WSEL predicted at the upstream boundary by the field-based rating relationship. In cases where the simulated WSELs at the highest simulation flow varied across the channel by more than 0.1 ft (0.031 m), the highest measured WSEL within the range of simulated flows for River2D calibration was used. The bed roughness heights of the computational mesh elements were modified by multiplying them by a constant bed roughness height multiplier until the WSELs predicted by River2D at the upstream end of the site matched the WSELs predicted by the field-based rating at the upstream

boundary cross section. The minimum groundwater depth was adjusted to a value of 0.05 m to increase the stability of the model. The values of all other River2D hydraulic parameters were left at their default values (upwinding coefficient = 0.5, groundwater transmissivity = 0.1, groundwater storativity = 1, and eddy viscosity parameters  $\epsilon_1 = 0.01$ ,  $\epsilon_2 = 0.5$  and  $\epsilon_3 = 0.1$ ).

The upstream boundary cross section was calibrated using the methods described above, varying the bed roughness multiplier until the simulated WSEL at the upstream boundary matched the measured WSEL at the upstream boundary. A stable solution generally has a solution change (Sol  $\Delta$ ) of less than 0.00001 and a net flow (Net Q) of less than 1% (Steffler and Blackburn 2002). WSELs predicted by the 2D model are expected to be within 0.1 ft (0.031 m) of the WSELs measured at the upstream cross section.<sup>f</sup>

Depth averaging models like River2D are most readily applied to subcritical stream conditions with, Froude Number (FN) of less than 1.0 (<1.0).<sup>g</sup> The maximum FN for a simulation is referred to as here as Max F. Max F is often used as a calibration tool to verify the simulated flow regime was subcritical and the water surface at any given point was stable. As stream gradients increase and/or large substrates are introduced to the stream bed, flow conditions transition from laminar (subcritical) to transient to turbulent with vertical mixing (supercritical). The FN is greater than 1.0 (i.e., >1.0) in supercritical conditions. Depths are more variable at any given point in supercritical conditions. River2D can predict depths in subcritical, supercritical, and transient conditions, but because of the variable water surface, predicted depths are less reliable than predictions made in subcritical areas. Max F <1.0. FN was computed along the shallowest course of each critical riffle at each simulation. Portions of the study site would be expected to have supercritical flows, based on the stream gradient and substrate sizes present in the site.

---

<sup>f</sup> We have selected this standard to comply with USFWS PHABSIM standards (USFWS 2011).

<sup>g</sup> This criterion is based on the assumption that flow in low gradient streams is usually subcritical (laminar), where the Froude number is less than 1.0.

## B.4 River2D WSEL Calibration Results

The River2D Pre-storm model required predictive WSEL-flow ratings be developed for the downstream boundary, XS-1, and the upstream boundary, XS-2, as seen in Figure 10 of the main report. The Pre-storm ratings were developed from data collected during the second half of January and the first half of February 2017. The data for the downstream boundary, XS-1, are presented in Table B-4 through B-10 and the data for the upstream boundary, XS-2, are presented in Table B-11 through B-14. Several storms were recorded at the Foster Park gage during this period in 2017 (Figure B-3). However, channel changes caused by the first storm, reflected in shifts in the rating curve, restricted the WSELs used to those from the first storm. The flow at the study site was estimated by subtracting the contribution from San Antonio Creek (Figure B-1) from the Foster Park data. The site flows estimated from the first storm in January 2017 were paired with the water level data recorded by the PTs installed along the boundary cross sections, XS-1, and XS-2.

**Table B-4.** Pre-storm XS-1 rating data 1. SZF at 309.1 ft.

Date	Time	Flow (cfs)	WSEL (ft)	LOG (Q)	LOG (WSEL-SZF)	Predicted LOG (WSEL-SZF)	Predicted WSEL (ft)	Error
1/21/2017	8:45	24.17	309.13	1.38	-1.49	-1.38	309.14	0.01
1/21/2017	8:30	24.86	309.16	1.40	-1.22	-1.30	309.15	0.01
1/21/2017	8:15	26.94	309.18	1.43	-1.07	-1.07	309.19	0.00
1/21/2017	8:00	27.63	309.22	1.44	-0.94	-0.99	309.20	0.01
1/21/2017	7:45	28.32	309.24	1.45	-0.84	-0.92	309.22	0.02
1/21/2017	7:30	30.39	309.27	1.48	-0.76	-0.72	309.29	0.02
1/21/2017	7:15	31.08	309.30	1.49	-0.69	-0.65	309.32	0.02

**Table B-5.** Pre-storm XS-1 rating data 2. SZF at 309.1 ft.

Date	Time	Flow (cfs)	WSEL (ft)	LOG (Q)	LOG (WSEL-SZF)	Predicted LOG (WSEL-SZF)	Predicted WSEL (ft)	Error
1/21/2017	7:00	33.15	309.34	1.52	-0.62	-0.62	309.34	0.00
1/21/2017	6:45	34.53	309.37	1.54	-0.57	-0.57	309.37	0.00
1/21/2017	6:30	35.92	309.40	1.56	-0.53	-0.52	309.40	0.00
1/21/2017	6:15	36.61	309.43	1.56	-0.48	-0.50	309.42	0.01
1/21/2017	6:00	37.99	309.45	1.58	-0.45	-0.45	309.46	0.00

**Table B-6.** Pre-storm XS-1 rating data 3. SZF at 309.1 ft.

Date	Time	Flow (cfs)	WSEL (ft)	LOG (Q)	LOG (WSEL-SZF)	Predicted LOG (WSEL-SZF)	Predicted WSEL (ft)	Error
1/21/2017	5:45	39.37	309.47	1.60	-0.43	-0.41	309.49	0.02
1/21/2017	5:15	42.13	309.50	1.62	-0.39	-0.38	309.51	0.01
1/21/2017	5:30	42.13	309.49	1.62	-0.41	-0.38	309.51	0.02
1/21/2017	5:00	43.51	309.52	1.64	-0.38	-0.37	309.53	0.01
1/21/2017	4:45	44.20	309.54	1.65	-0.36	-0.37	309.53	0.01
1/21/2017	4:30	44.89	309.55	1.65	-0.35	-0.36	309.54	0.01
1/21/2017	4:15	46.97	309.57	1.67	-0.33	-0.34	309.55	0.02
1/21/2017	4:00	47.66	309.58	1.68	-0.32	-0.34	309.56	0.03
1/21/2017	3:30	50.42	309.60	1.70	-0.30	-0.32	309.58	0.02
1/21/2017	3:45	50.42	309.59	1.70	-0.31	-0.32	309.58	0.01
1/21/2017	3:15	51.11	309.62	1.71	-0.28	-0.31	309.59	0.03
1/21/2017	2:45	54.56	309.64	1.74	-0.27	-0.29	309.61	0.02
1/21/2017	3:00	54.56	309.63	1.74	-0.27	-0.29	309.61	0.02
1/21/2017	2:30	57.33	309.65	1.76	-0.26	-0.27	309.63	0.01
1/21/2017	2:00	58.02	309.65	1.76	-0.26	-0.27	309.64	0.01
1/21/2017	1:15	59.40	309.57	1.77	-0.33	-0.26	309.65	0.08
1/21/2017	2:15	59.40	309.65	1.77	-0.26	-0.26	309.65	0.01
1/21/2017	1:45	61.47	309.64	1.79	-0.27	-0.25	309.67	0.03
1/21/2017	1:00	62.16	309.64	1.79	-0.27	-0.24	309.67	0.03
1/21/2017	1:30	62.16	309.59	1.79	-0.31	-0.24	309.67	0.08
1/21/2017	0:45	67.00	309.73	1.83	-0.20	-0.22	309.71	0.02
1/21/2017	0:30	71.83	309.83	1.86	-0.14	-0.19	309.74	0.08

**Table B-7.** Pre-storm XS-1 rating data 4. SZF at 309.1 ft.

Date	Time	Flow (cfs)	WSEL (ft)	LOG (Q)	LOG (WSEL-SZF)	Predicted LOG (WSEL-SZF)	Predicted WSEL (ft)	Error
1/21/2017	0:15	81.50	309.90	1.91	-0.10	-0.15	309.82	0.09
1/21/2017	0:00	87.02	309.91	1.94	-0.09	-0.12	309.86	0.06
1/20/2017	23:45	91.86	309.94	1.96	-0.08	-0.09	309.92	0.02
1/20/2017	23:30	96.69	309.93	1.99	-0.08	-0.09	309.92	0.00
1/20/2017	23:15	99.46	309.93	2.00	-0.08	-0.08	309.92	0.01
1/20/2017	23:00	101.53	309.93	2.01	-0.08	-0.08	309.92	0.01
1/20/2017	22:45	107.05	309.93	2.03	-0.08	-0.08	309.93	0.00
1/20/2017	22:30	109.82	309.90	2.04	-0.10	-0.08	309.93	0.02

**Table B-8.** Pre-storm XS-1 rating data 5. SZF at 309.1 ft.

<b>Date</b>	<b>Time</b>	<b>Flow (cfs)</b>	<b>WSEL (ft)</b>	<b>LOG (Q)</b>	<b>LOG (WSEL -SZF)</b>	<b>Predicted LOG (WSEL -SZF)</b>	<b>Predicted WSEL (ft)</b>	<b>Error</b>
1/20/2017	20:15	147.80	310.14	2.17	0.02	0.03	310.17	0.03
1/20/2017	20:00	158.16	310.25	2.20	0.06	0.07	310.27	0.02
1/20/2017	19:45	174.05	310.49	2.24	0.14	0.12	310.42	0.07
1/20/2017	18:30	194.77	310.65	2.29	0.19	0.18	310.62	0.02
1/20/2017	19:30	194.77	310.65	2.29	0.19	0.18	310.62	0.03
1/20/2017	18:15	200.30	310.72	2.30	0.21	0.20	310.68	0.04
1/20/2017	19:15	212.73	310.80	2.33	0.23	0.23	310.81	0.01
1/20/2017	18:00	218.94	310.79	2.34	0.23	0.25	310.87	0.08
1/20/2017	19:00	225.16	310.92	2.35	0.26	0.26	310.93	0.02

**Table B-9.** Pre-storm XS-1 rating data 6. SZF at 309.1 ft.

Date	Time	Flow (cfs)	WSEL (ft)	LOG (Q)	LOG (WSEL -SZF)	Predicted LOG (WSEL -SZF)	Predicted WSEL (ft)	Error
1/20/2017	17:45	238.28	310.87	2.38	0.25	0.26	310.91	0.04
1/20/2017	17:30	247.26	310.95	2.39	0.27	0.26	310.94	0.01
1/20/2017	17:15	278.34	311.04	2.44	0.29	0.29	311.04	0.00
1/20/2017	17:00	309.42	311.14	2.49	0.31	0.31	311.13	0.01
1/20/2017	16:45	357.08	311.25	2.55	0.33	0.33	311.26	0.01
1/20/2017	16:30	402.66	311.35	2.60	0.35	0.36	311.38	0.03
1/20/2017	16:15	448.94	311.45	2.65	0.37	0.38	311.49	0.03
1/20/2017	16:00	502.81	311.60	2.70	0.40	0.40	311.61	0.00
1/20/2017	15:45	551.85	311.74	2.74	0.42	0.42	311.71	0.03
1/20/2017	15:30	604.34	311.91	2.78	0.45	0.43	311.82	0.10
1/20/2017	15:15	718.30	312.11	2.86	0.48	0.47	312.03	0.09
1/20/2017	15:00	904.78	312.36	2.96	0.51	0.51	312.34	0.03
1/20/2017	14:45	1167.24	312.68	3.07	0.55	0.56	312.72	0.03
1/20/2017	14:30	1457.32	312.96	3.16	0.59	0.58	312.89	0.07

**Table B-10.** Pre-storm XS-1 rating data 7. SZF at 309.1 ft.

Date	Time	Flow (cfs)	WSEL (ft)	LOG (Q)	LOG (WSEL -SZF)	Predicted LOG (WSEL -SZF)	Predicted WSEL (ft)	Error
1/20/2017	14:15	1761.22	313.30	3.25	0.62	0.62	313.29	0.01
1/20/2017	14:00	2120.37	313.72	3.33	0.66	0.67	313.73	0.00
1/20/2017	13:45	2520.96	314.11	3.40	0.70	0.71	314.18	0.06
1/20/2017	12:45	2569.31	314.24	3.41	0.71	0.71	314.23	0.01
1/20/2017	13:00	2762.70	314.51	3.44	0.73	0.73	314.43	0.08
1/20/2017	13:30	2831.76	314.51	3.45	0.73	0.73	314.50	0.01
1/20/2017	13:15	2949.18	314.58	3.47	0.74	0.74	314.62	0.04

**Table B-11.** Pre-storm XS-2 rating data 1. SZF at 388.7 ft.

Date	Time	Flow (cfs)	WSEL (ft)	LOG (Q)	LOG (WSEL -SZF)	Predicted LOG (WSEL -SZF)	Predicted WSEL (ft)	Error
1/20/2017	10:45	0.90	388.76	-0.05	-1.32	-1.32	388.76	0.00
1/20/2017	19:45	108.68	389.84	2.04	0.05	0.03	389.78	0.06
1/20/2017	17:45	200.30	390.23	2.30	0.18	0.18	390.22	0.01

**Table B-12.** Pre-storm XS-2 rating data 2. SZF at 388.7 ft.

Date	Time	Flow (cfs)	WSEL (ft)	LOG (Q)	LOG (WSEL -SZF)	Predicted LOG (WSEL -SZF)	Predicted WSEL (ft)	Error
1/20/2017	17:30	218.94	390.28	2.34	0.20	0.20	390.29	0.01
1/20/2017	17:15	238.28	390.34	2.38	0.21	0.22	390.36	0.01
1/20/2017	17:00	247.26	390.41	2.39	0.23	0.23	390.39	0.02

**Table B-13.** Pre-storm XS-2 rating data 3. SZF at 388.7 ft.

Date	Time	Flow (cfs)	WSEL (ft)	LOG (Q)	LOG (WSEL-SZF)	Predicted LOG (WSEL-SZF)	Predicted WSEL (ft)	Error
1/20/2017	16:45	278.34	390.47	2.44	0.25	0.25	390.47	0.00
1/20/2017	16:30	309.42	390.54	2.49	0.26	0.26	390.53	0.01
1/20/2017	16:15	357.08	390.61	2.55	0.28	0.28	390.62	0.00
1/20/2017	16:00	402.66	390.69	2.60	0.30	0.30	390.69	0.01
1/20/2017	15:45	448.94	390.75	2.65	0.31	0.31	390.76	0.01
1/20/2017	15:30	502.81	390.82	2.70	0.33	0.33	390.84	0.01
1/20/2017	15:15	551.85	390.89	2.74	0.34	0.34	390.90	0.01
1/20/2017	15:00	604.34	390.99	2.78	0.36	0.35	390.96	0.03
1/20/2017	14:45	718.30	391.09	2.86	0.38	0.38	391.09	0.00

**Table B-14.** Pre-storm XS-2 rating data 4. SZF at 388.7 ft.

Date	Time	Flow (cfs)	WSEL (ft)	LOG (Q)	LOG (WSEL-SZF)	Predicted LOG (WSEL-SZF)	Predicted WSEL (ft)	Error
1/20/2017	14:30	904.78	391.20	2.96	0.40	0.40	391.20	0.00
1/20/2017	14:15	1167.24	391.34	3.07	0.42	0.42	391.36	0.02
1/20/2017	14:00	1457.32	391.47	3.16	0.44	0.45	391.51	0.04
1/20/2017	13:45	1761.22	391.62	3.25	0.46	0.47	391.65	0.03
1/20/2017	12:00	1864.82	391.75	3.27	0.48	0.47	391.69	0.06
1/20/2017	13:30	2120.37	391.78	3.33	0.49	0.49	391.79	0.00
1/20/2017	13:15	2520.96	391.94	3.40	0.51	0.51	391.92	0.02
1/20/2017	12:15	2569.31	391.90	3.41	0.50	0.51	391.94	0.04
1/20/2017	12:30	2762.70	392.02	3.44	0.52	0.52	391.99	0.03

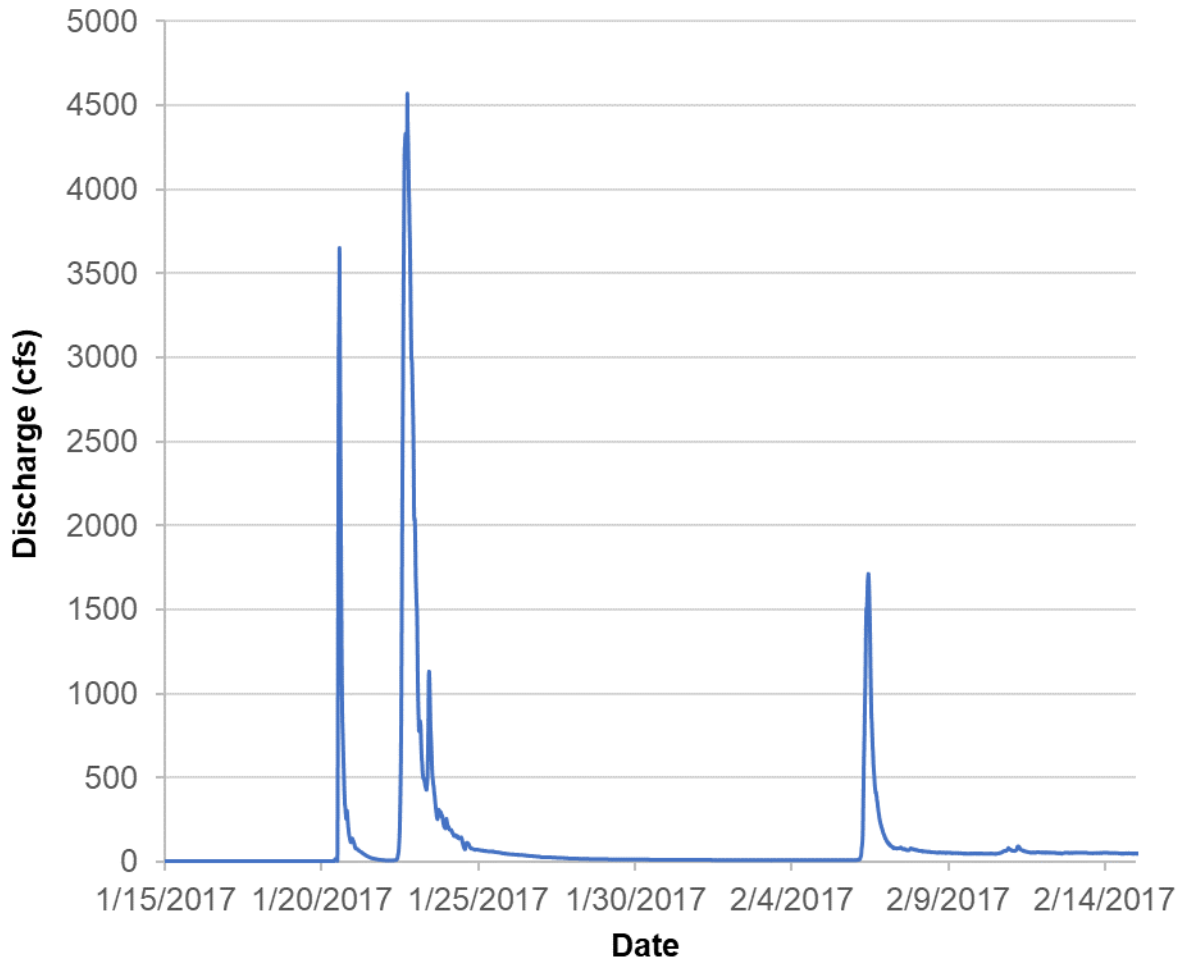


**Figure B-3.** 15-minute hydrograph from USGS gage 11118500 at Foster Park from 1/15/2017 through 2/14/2017.

At the onset of the study, the range of flows required to evaluate adult steelhead passage were unknown. Findings of a previous passage study prepared for the Casitas Municipal Water District (CMWD 2010) indicated flow levels needed to be evaluated up to 3,000 cfs. Because flows were simulated over a wide range, changes in the cross-sectional area of the boundary cross sections required the rating to be partitioned into a series of linear segments (Figure B-4; USGS 2001). The area of the cross section corresponding to each rating segments is shown in Figure B-5. The segments generally broke near transitions in the right bank slope, as the left bank slope grade was more uniform. The correlation coefficients ( $R^2$ ) of each rating relationship segment are provided in Table B-15.

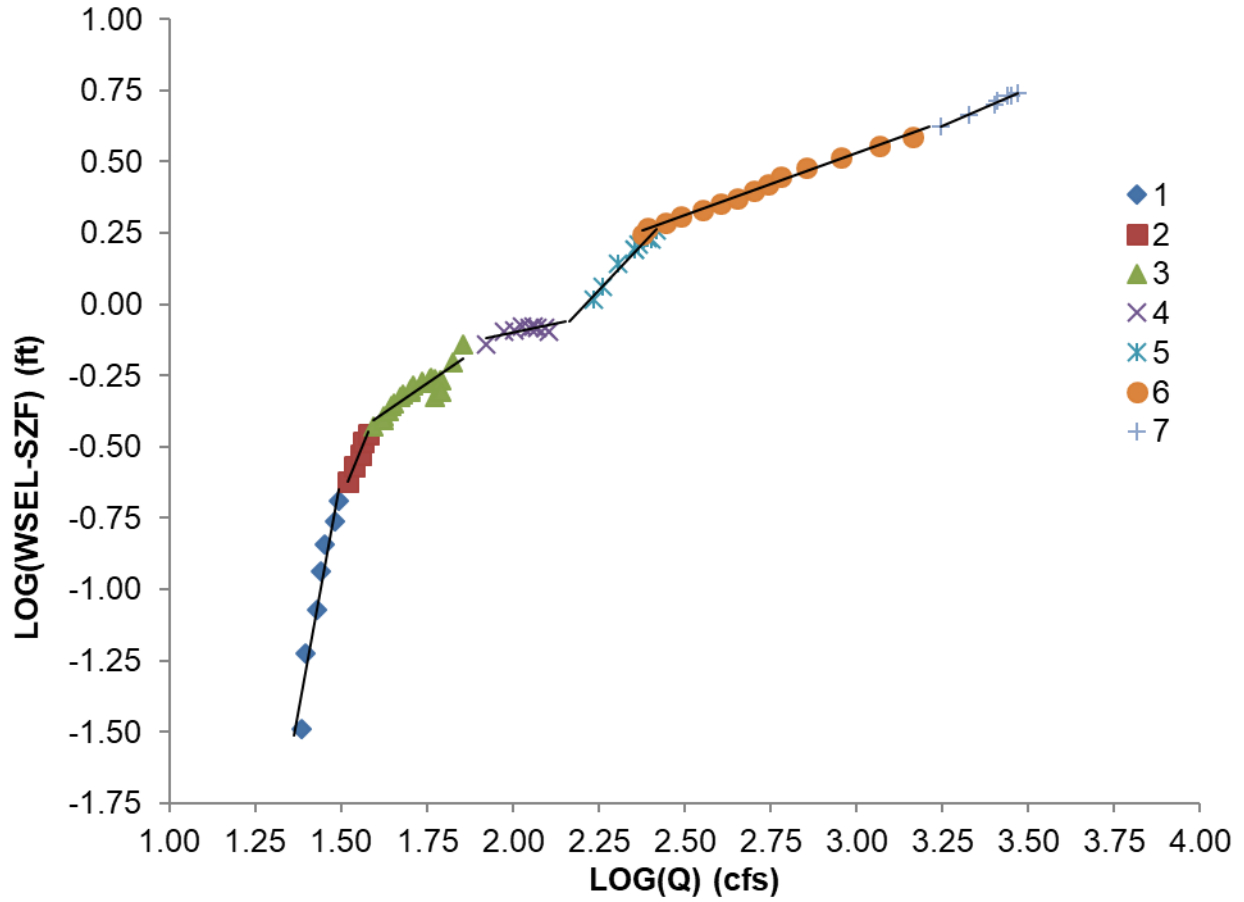


**Figure B-4.** Pre-storm XS-1 WSEL-flow rating curve, with each linear segment at changes in the cross section.

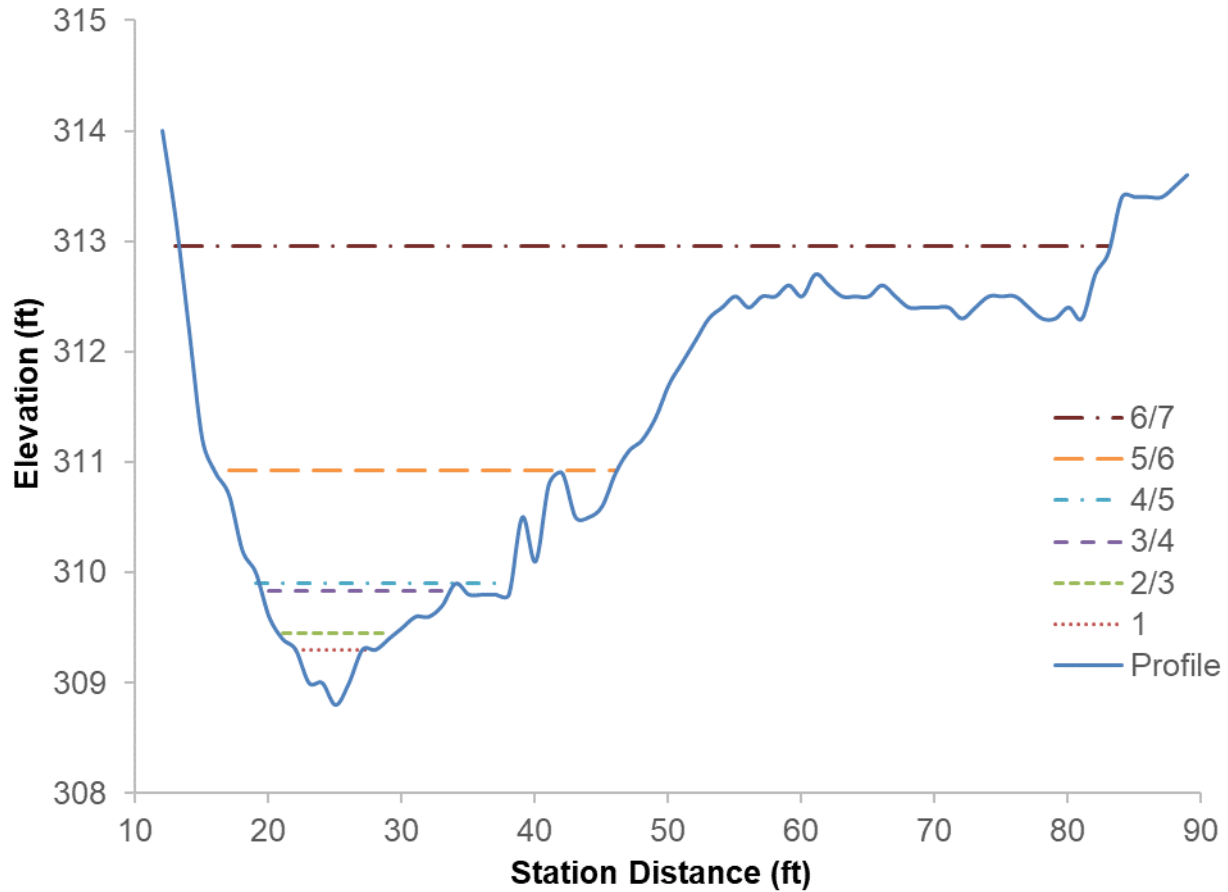


**Figure B-5.** Pre-storm XS-1 rating curve segments at the cross section bed profile. Each rating curve breakline indicates changes within the cross section.

**Table B-15.** River2D XS-1 WSEL calibration R2 values.

Segment	Flow Range	R <sup>2</sup>
1	Q < 33.2 cfs	0.936
2	33.2 cfs < Q < 38 cfs	0.988
3	38 cfs < Q < 71.8 cfs	0.815
4	71.8 cfs < Q < 109.8 cfs	0.059
5	109.8 cfs < Q < 225.2 cfs	0.975
6	225.2 cfs < Q < 1,457.3 cfs	0.994
7	1,457.3 cfs < Q < 2,949.2 cfs	0.992

The rating curve for XS-2 only required four segments (Figure B-6). The WSEL of the segment breaks within the cross section profile are shown in Figure B-7. The R<sup>2</sup> values for Pre-storm XS-2 rating were all above 98% (Table B-16).

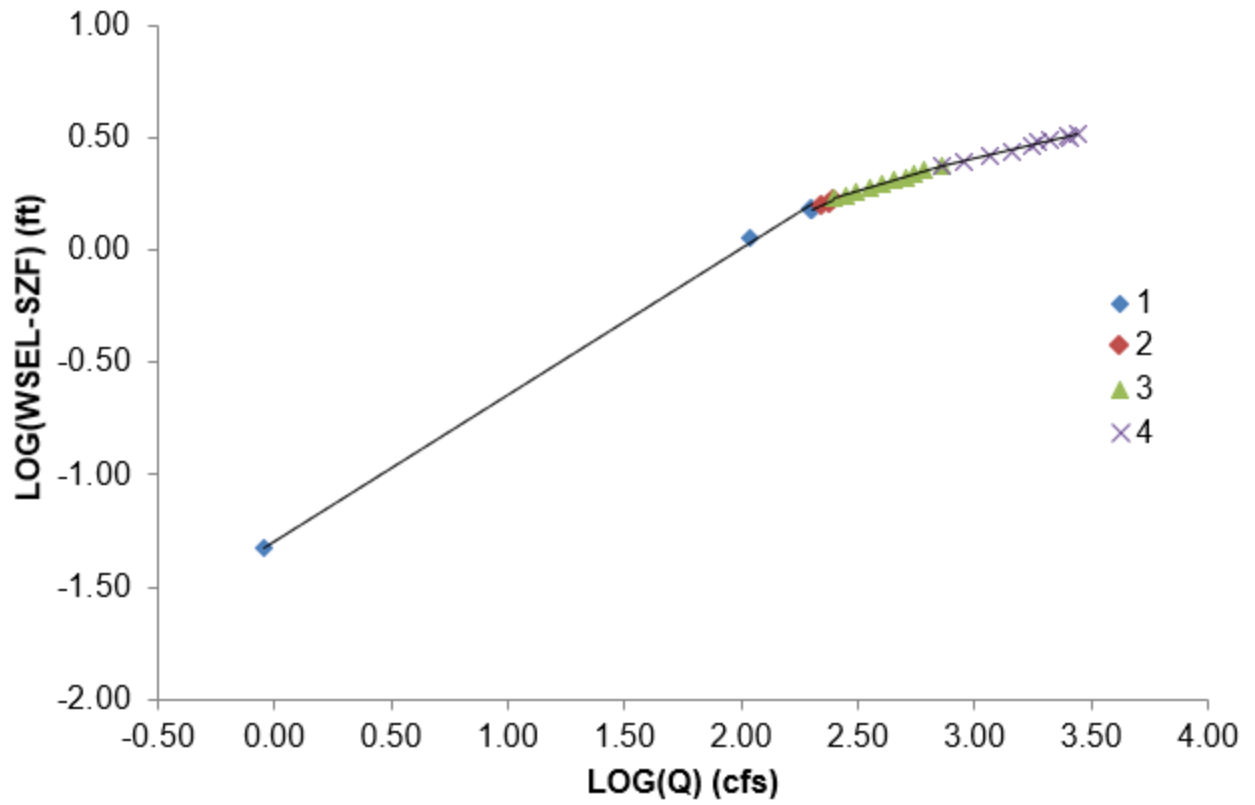


**Figure B-6.** Pre-storm XS-2 WSEL-flow rating curve, with each linear segment at changes in the cross section.

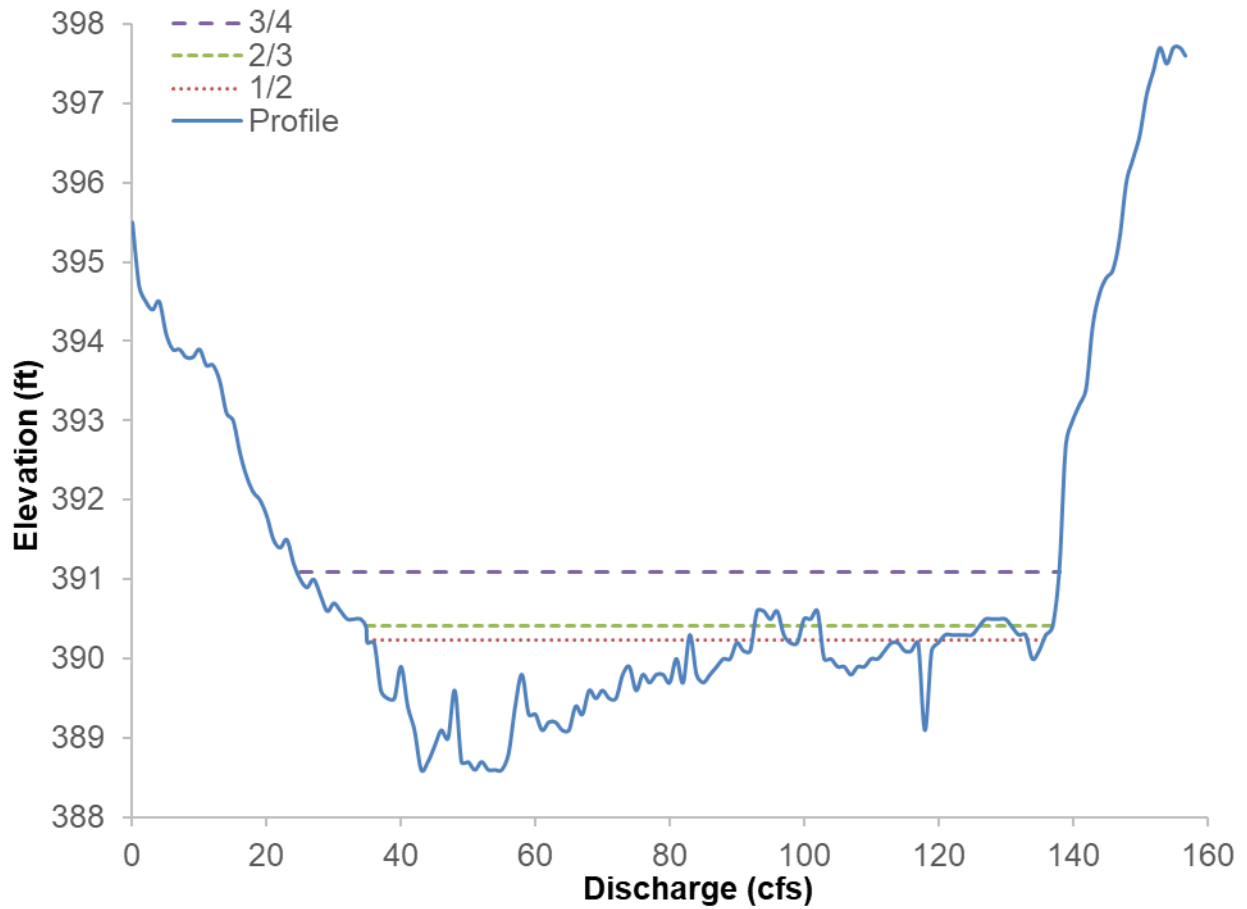


**Figure B-7.** Pre-storm XS-2 profile and rating segments.

**Table B-16.** River2D XS-2 WSEL calibration  $R^2$  values.

Segment	Flow Range	$R^2$
1	$Q < 219$ cfs	0.999
2	$219$ cfs $< Q < 278$ cfs	0.966
3	$278$ cfs $< Q < 905$ cfs	0.998
4	$905$ cfs $< Q < 2,763$ cfs	0.989

## B.5 River2D Model Construction Results

River2D model construction was performed using ArcView GIS and the R2D\_BED and R2D\_MESH utility programs. ArcView was used to view and organize the field survey points collected using the RTK GPS and total station. The LIDAR points from the 2005 flight were imported into ArcView to fill areas that could not be completed by the field survey. These areas typically included steep banks, flood plains, and private property located near the channel. Polygons were drawn around the boundary of the field survey points; the LIDAR points within the area of the field survey were removed. Figure B-8 provides an example of the interface between the surveyed points and the LIDAR points.

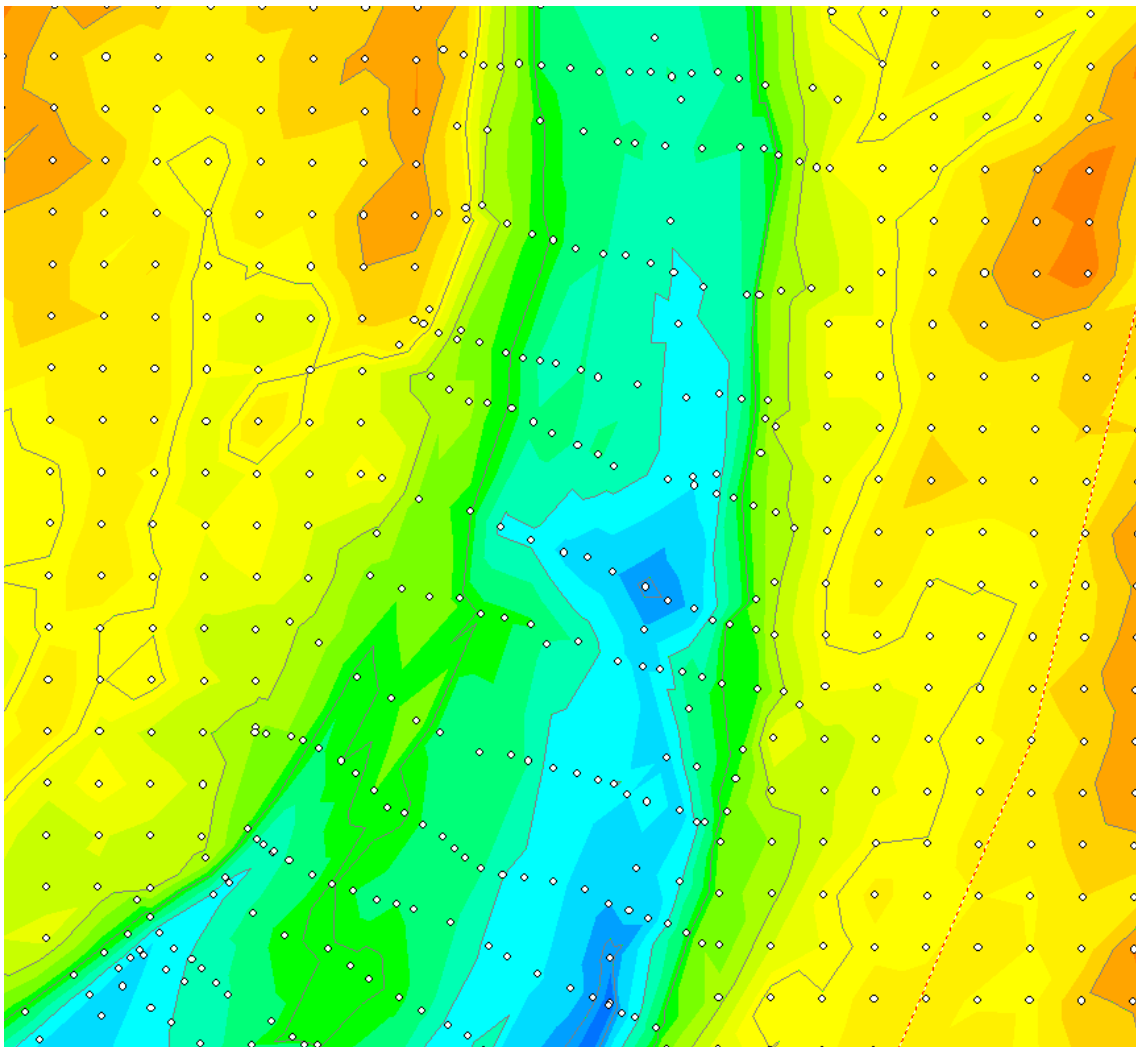


**Figure B-8.** Interface of field survey points and LIDAR points using River2D. All points shown as white dots over bed elevation. Field survey points were collected in transects. LIDAR points are in a regular 3-m grid pattern.

The survey and LIDAR points were gathered into a single text file and imported into the R2D\_BED utility program. A total 11,786 survey points and 34,191 LIDAR points were imported into the R2\_BED program. The external boundary was added, after which internal boundaries were added separating the main channel bed and banks from the flood plain. The flow simulation area was confined to areas inundated at 3,000 cfs. The bed topography points were reviewed using the program display settings to check for erroneous point elevations. The bed program can be set to display elevation contour lines at predetermined intervals and elevation gradient by color shading. Confined clusters of contour lines and sharp color contrasts indicated a point elevation was different from the point's nearest neighbors. A total of 11,786 points were collected using the RTK GPS and the total station. A total of 22 points were found to have erroneous elevations that could not be corrected by adjusting the total station rod height or RTK pole height and were removed from the bed file. A total of 22,072 breakline segments were added to the bed file, generating 44,988 additional synthetic nodes to the bed file, for a total of 90,965 nodes.

Once the bed topography, flow boundaries, and breaklines were defined in the bed program, the completed bed file was moved into the mesh utility. An initial, uniformly spaced triangular mesh was applied to the bed file. The uniform mesh was refined by adding mesh breaklines and increasing the mesh density in areas with complex hydraulics or rapid elevation changes. The mesh was refined until an acceptable QI value was reached, equal to or greater than 0.2. The final QI value for the Pre-storm River2D mesh was 0.3. Once the mesh was completed, the bed and mesh files were imported into River2D creating the .cdg file used for flow simulation. The computational mesh nodes were exported from River2D and the elevations of the computational mesh nodes were compared to the bed file nodes. The percent of computational mesh nodes within 0.1 ft of the bed files nodes was 77%.

## **B.6 River2D Model Calibration Results**

The Pre-storm model calibration began at a highest simulated flow of 3,000 cfs. Seven flow simulations were run for the fish passage analysis as follows: 400 cfs, 300 cfs, 250 cfs, 200 cfs, 150 cfs, 100 cfs and 50 cfs. The WSEL/flow calibration results for the simulations used to evaluate the critical riffles are provided in Table B-17. The simulation execution parameters and output statistics including bed roughness multiplier, solution change at the end of the last simulation timestep, difference in Net Q between the boundary cross sections, and the mean and maximum FN for each flow simulation are provided in Table B-18.

The calibration performance was measured by comparing the differences of the final simulation runs with either the field-based flow-WSEL calibration data or guidance thresholds described in the methods section. A bed roughness multiplier of 0.3 was

used for each flow simulation from 50 cfs to 400 cfs. Bed roughness multipliers below 0.3 are not considered to be reasonable for a riverine open channel. The WSEL calibration information for the flow simulations executed is presented in Table B-17. The simulated WSELs measured at the upstream boundary cross sections (XS-2) were not within 0.1 ft (0.031 m) of the field-based rating WSELs. The simulated WSELs between 400 cfs and 200 cfs ranged from 0.35 ft to 0.32 ft or approximately 0.1 m. The difference in simulated versus rating-predicted WSEL increased with each decreasing flow simulation. The WSEL variance was 0.68 ft at the lowest flow simulation, 50 cfs.

The discrepancy in simulated versus rated WSEL is most likely due to a shift in the flow-WSEL rating relationship caused by the initial peak flood flow of 3,650 cfs on January 20, 2017 prior to the large-scale event starting on February 17, 2017 (Figures A-1 and B-3). The flow-WSEL rating was generated from the flows reported by USGS at the Foster Park stream gage minus San Antonio Creek flows, and WSELs converted from PT measurements on the receding limb of the initial storm described above. The ascending limb of the initial storm rose too fast to have any WSELs that could be used to develop a rating curve. The model DTM was created from survey data collected prior to the January 2017 storm. The XS-2 bed elevation profile was measured in October 2016, and then again in April 2017 (Figure B-9). The differences in the bed elevation profile shown in Figure B-9 cannot be exclusively linked to the initial storm in January because several more storm events occurred before the April 2017 survey (Figures A-1 and B-3). The increase in WSEL variance as simulation flows decreased indicates that the flow-WSEL rating may have also been impacted by changes to the location and bed elevation of the downstream control point, SZF.

**Table B-17.** Pre-storm boundary cross section WSEL/flow simulation results.

Flow (cfs)	XS-2 WSEL (ft) Field Rating	XS-2 WSEL (ft) River2D	XS-2 WSEL (ft) (+/-)
400	390.69	391.02	0.34
350	390.60	390.96	0.35
300	390.51	390.86	0.35
250	390.40	390.75	0.35
200	390.30	390.62	0.32
150	390.03	390.46	0.43
100	389.72	390.26	0.54
50	389.36	390.04	0.68

The other model calibration performance criteria are summarized in Table B-18. The minimum bed roughness multiplier of 0.3 was required to minimize the variance in

simulated WSEL at XS-2. The solution change at the end of each final flow simulation file was for was below the standard of 0.00001. Net Q is the difference between the flow entering the upstream boundary versus exiting the downstream boundary and is recommended to be <1%. The Net Q for the simulations from 400 to 250 cfs met or came close to meeting the guidance. The flow simulation of 200 cfs at 3% was still within the USGS gage accuracy of 5%, but then the remaining simulations of 150 cfs to 50 cfs far exceeded the threshold. The pattern of Net Q followed the variance in WSEL (Table B-17). The River2D model performed better with respect to the standard calibration guidance at the higher simulated flows. At low flows, the model was not able to force the entire flow through the reduced downstream cross-sectional area, resulting in the high Net Q. This was likely due to a shift in the XS-1 rating curve caused by the initial storm, similar to the effect described above for XS-2. This phenomenon would not be expected to have any effect on model performance except near the downstream boundary.

**Table B-18.** Pre-storm simulation execution parameter and output statistics results.

Flow (cfs)	Bed Roughness Multiplier	Sol $\Delta$	Flow (cms)	Net Q (cms)	Net Q/Flow	Mean FN	Max FN
400	0.3	0.0000002	11.327	0.103	0.9%	0.37	5.11
300	0.3	0.0000050	8.495	0.1056	1.2%	0.33	11.31
250	0.3	0.0000020	7.079	0.1042	1.5%	0.30	7.28
200	0.3	0.0000010	5.663	0.168	3%	0.27	3.86
150	0.3	0.0000010	4.248	0.4723	11%	0.25	5.68
100	0.3	0.0000010	2.832	0.5333	19%	0.20	9.12
50	0.3	0.0000060	1.416	0.305	21%	0.14	14.8



**Figure B-9.** XS-2 bed elevation profiles before and after the 2016-2017 winter storms.

FN is a display option in River2D and was reviewed for each flow simulation. FN values for each flow simulation were exported from River2D. The average FN for each flow simulation was below 1.0. Maximum FN values in excess of 1.0 were found in isolated pockets around the boundaries of large substrates and bank margins (Figure B-10).

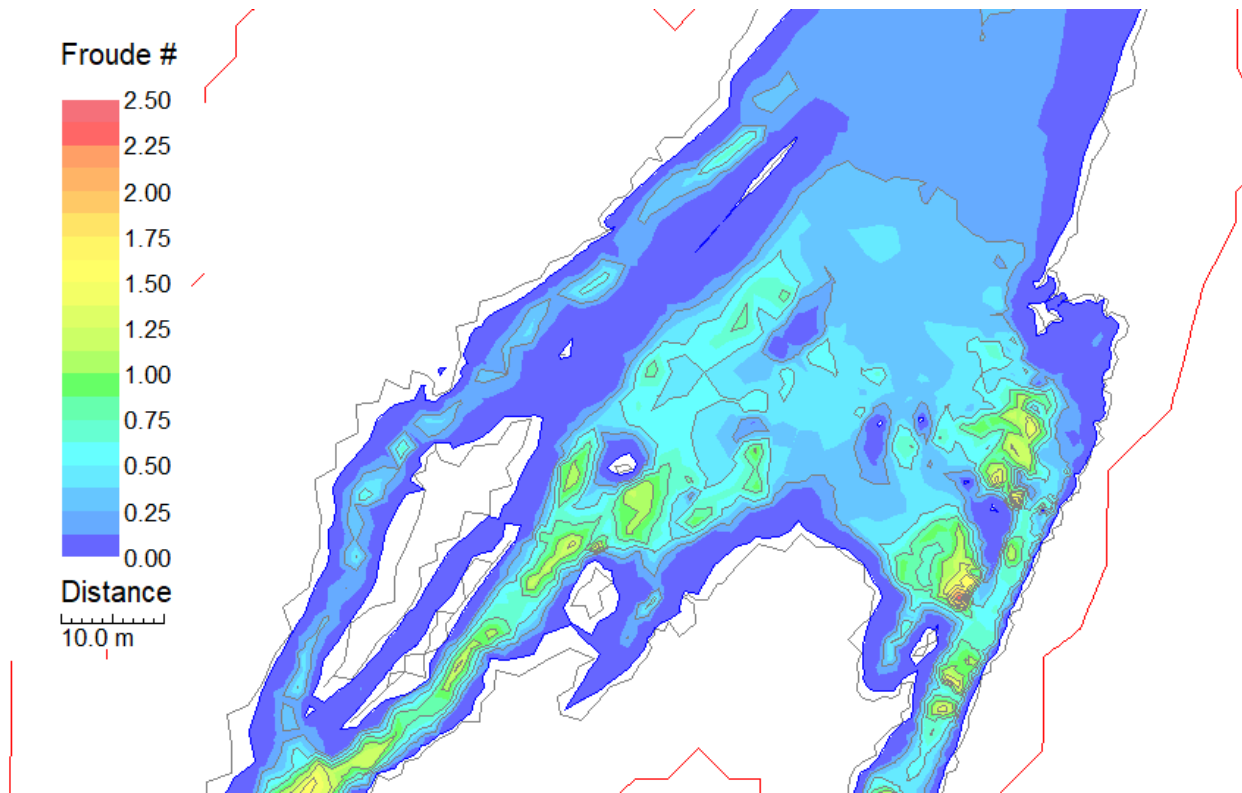


**Figure B-10.** River2D FN display of R23 at 200 cfs in the Pre-storm model.

Figure B-10 shows passage impediment site R23 at 200 cfs. There are FN values that exceed 1.0 around a cobble bar in the lower portion of the riffle site. Figure B-11 shows the water depth at the same location. Depths in and around the cobble bar are above and below the passage criterion of 0.7 ft (0.213 m) for adult steelhead. Fish passage is expected to be around the cobble bar where depths exceed the passage criteria and FNs are at up to 1.0.

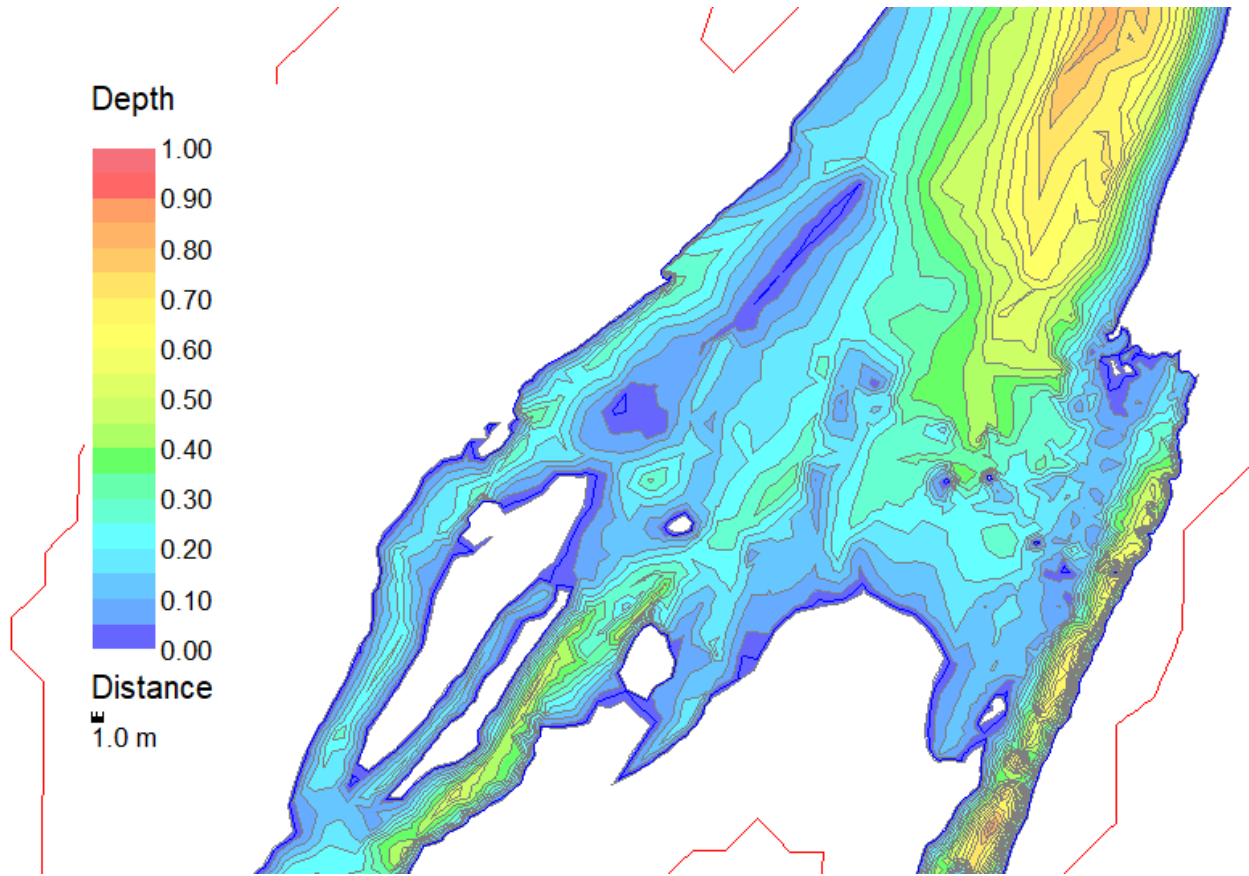


**Figure B-11.** River2D Depth (m) display at R23 at 200 cfs in the Pre-storm model.

## **APPENDIX C: HEC-RAS POST-STORM MODEL**

This Appendix presents the HEC-RAS (HEC-RAS 2018) model calibration methods and results for the Post-storm two-dimensional (2D) model created to evaluate passage conditions for upstream migration of adult steelhead through the intermittent reach of the Ventura River. This section presents the results of the WSEL calibration at the model boundary cross sections, the calibration of simulated versus measured hydraulic data within each model simulation, and hydraulic parameter settings used to achieve convergence of the model simulation results with the hydraulic data measured in the field.

### **C.1 HEC-RAS Flow-WSEL Calibration Methods**

After the February 2017 storm, boundary conditions were reestablished at the upstream and downstream ends of the intermittent reach study site. The upstream boundary cross section (XS-2) was reused because the channel was still single thread and banks were still in place at that location in the river channel. The downstream cross section (XS-1) was moved downstream approximately 80 m because the channel had braided in the original XS-1 location and reconnected into a single-thread channel further downstream, as seen in Figure 11 in the main report. On April 4, 2017, PTs were re-installed in the streambed along XS-1 and XS-2. On April 5 and 6 of 2017 the aforementioned critical riffle survey was performed. Random water depth model validation measurements were collected on April 5 at a flow of approximately 17 cfs. Topographic surveys commenced in November 2017 and were completed in June 2018. There were two major storm events in the 2018 water year, one in January and one in March (Figure C-1). Staff arrived in May 2018 to recover the PTs and use the data to develop the flow-WSEL rating relationship for the Post-storm model calibration. The PTs at the downstream boundary cross section were intact and recovered. The PT at XS-2 could not be located.

A flow-WSEL relationship was developed at XS-1 using the same method as the Pre-storm model. The first storm of the 2018 water year started in the morning of 1/9/2018 and lasted through midday on January 11, 2018 (Figure C-2). The PT data was plotted versus the stage data at Foster Park during a condensed period of the storm from approximately 7:00 AM to 7:30 PM (Figure C-3). When comparing the peaks in the USGS stage versus the PT level there was a half-hour lag between the PT at XS-1 and the USGS stream gage at Foster Park. The lag in time between when the PT level and USGS stage data was accounted for in the development of the flow-WSEL rating relationship. The XS-1 water level data was shifted in time to align with the flow peaks recorded at Foster Park.

Without the PT data at the upstream cross section (XS-2), a flow-WSEL relationship was developed using existing discharge and WSEL measurements and several more discharge and WSEL measurements recorded once the loss of the upstream PT was discovered. Several discharge-WSEL pairs were recorded in 2019 up to and during the first major storm in January 2019 (Figure C-4).

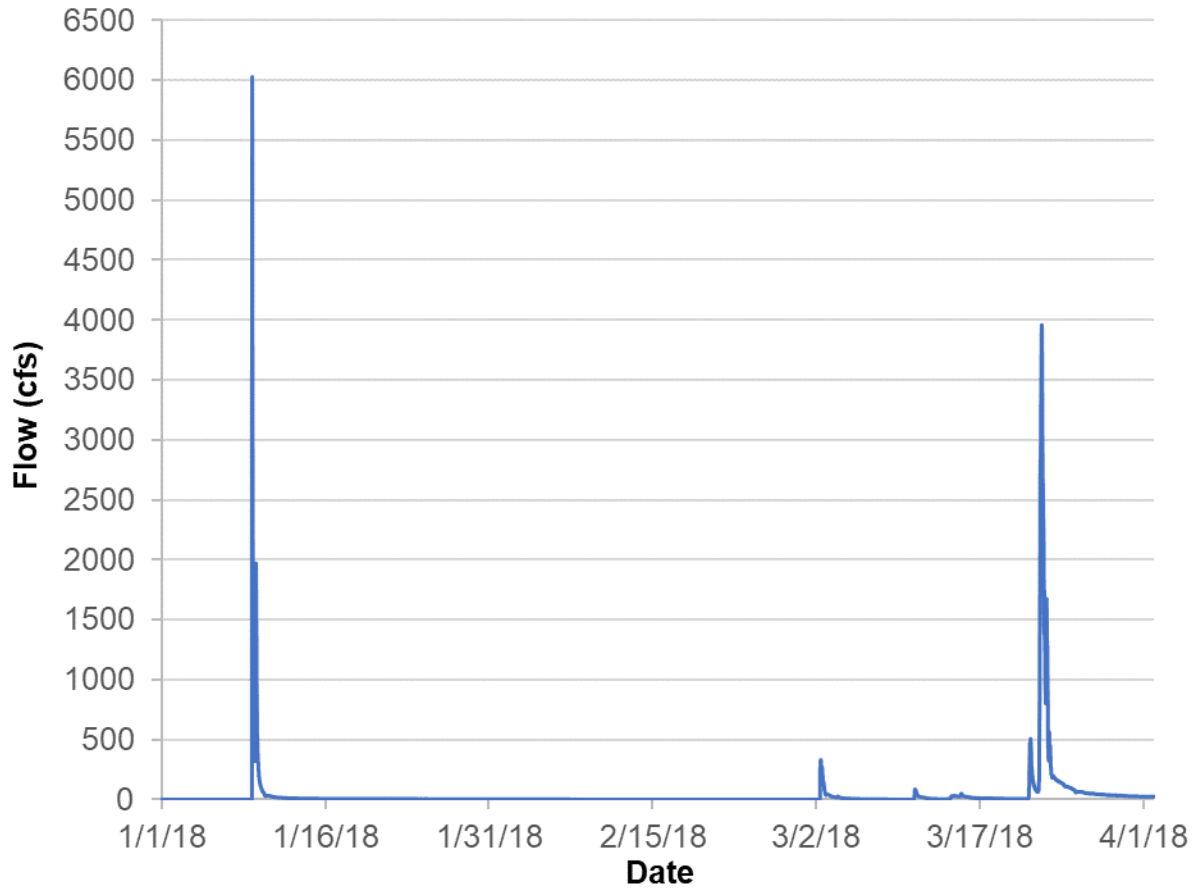


**Figure C-1.** Hydrograph of 2018 water year storms. 15-minute data provided by USGS 11118500, located near Foster Park, from 1/1/2018 to 4/1/2018.

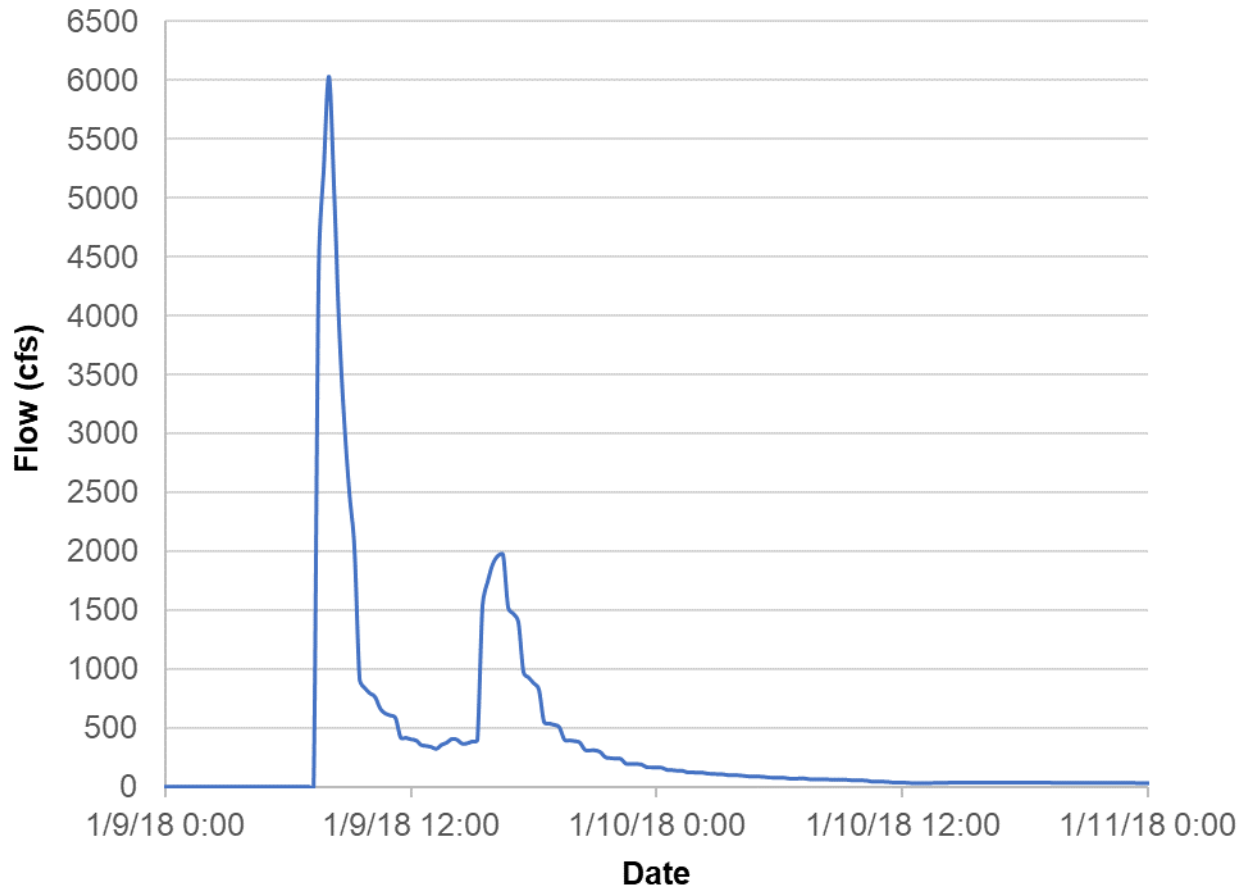


**Figure C-2.** 15-minute data provided by USGS 11118500, located near Foster Park, used to calibrate the Post-storm 2D model from 1/9/2018 12:00 AM to 1/11/2018 12:00 AM.

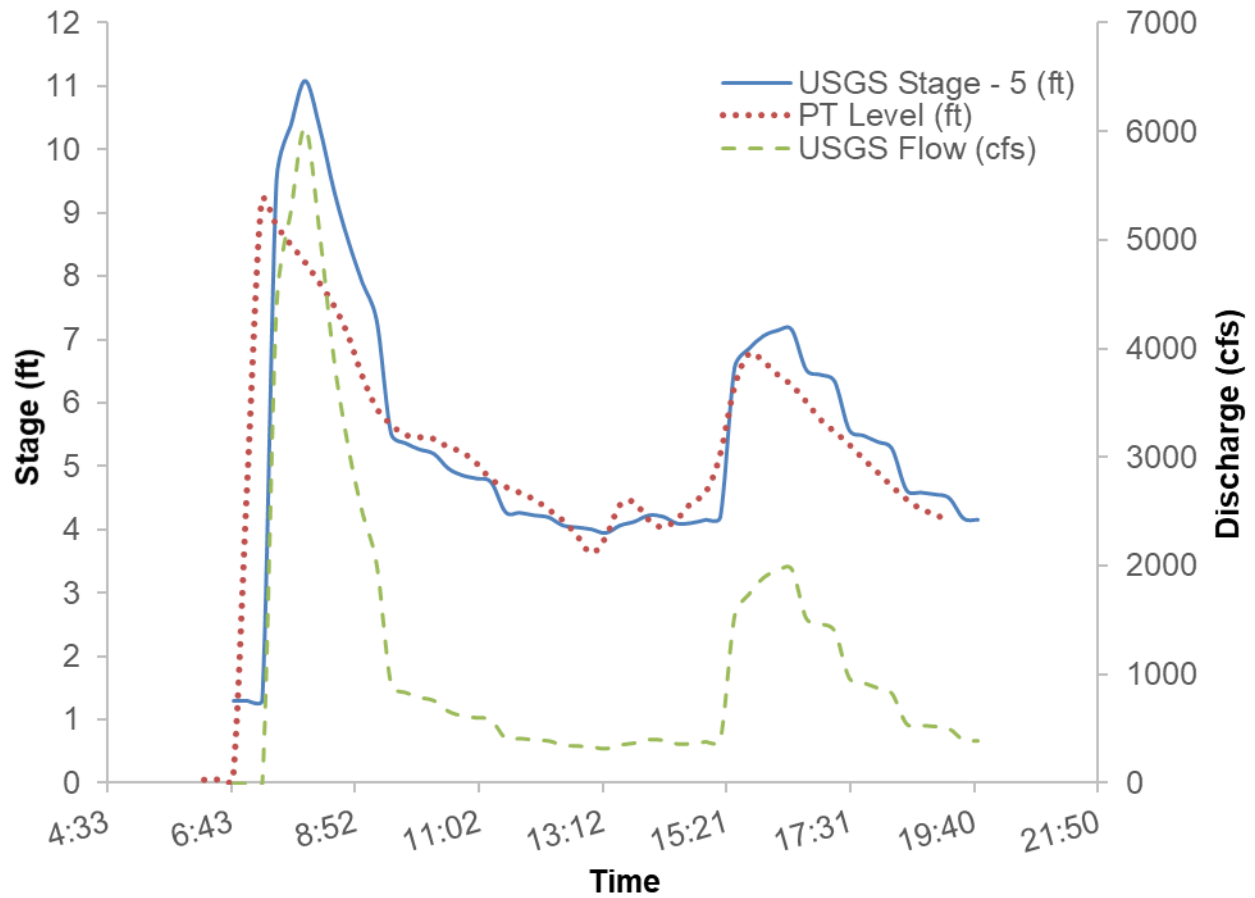


**Figure C-3.** Timing of water stage recorded at USGS 11118500, located near Foster Park, versus water level measured by the PT located in the Post-storm 2D flow area boundary cross section on January 9, 2018. Stage at the two locations are referenced to different datums. The stages reported by USGS were adjusted down by 5 ft to make the data easier to compare.

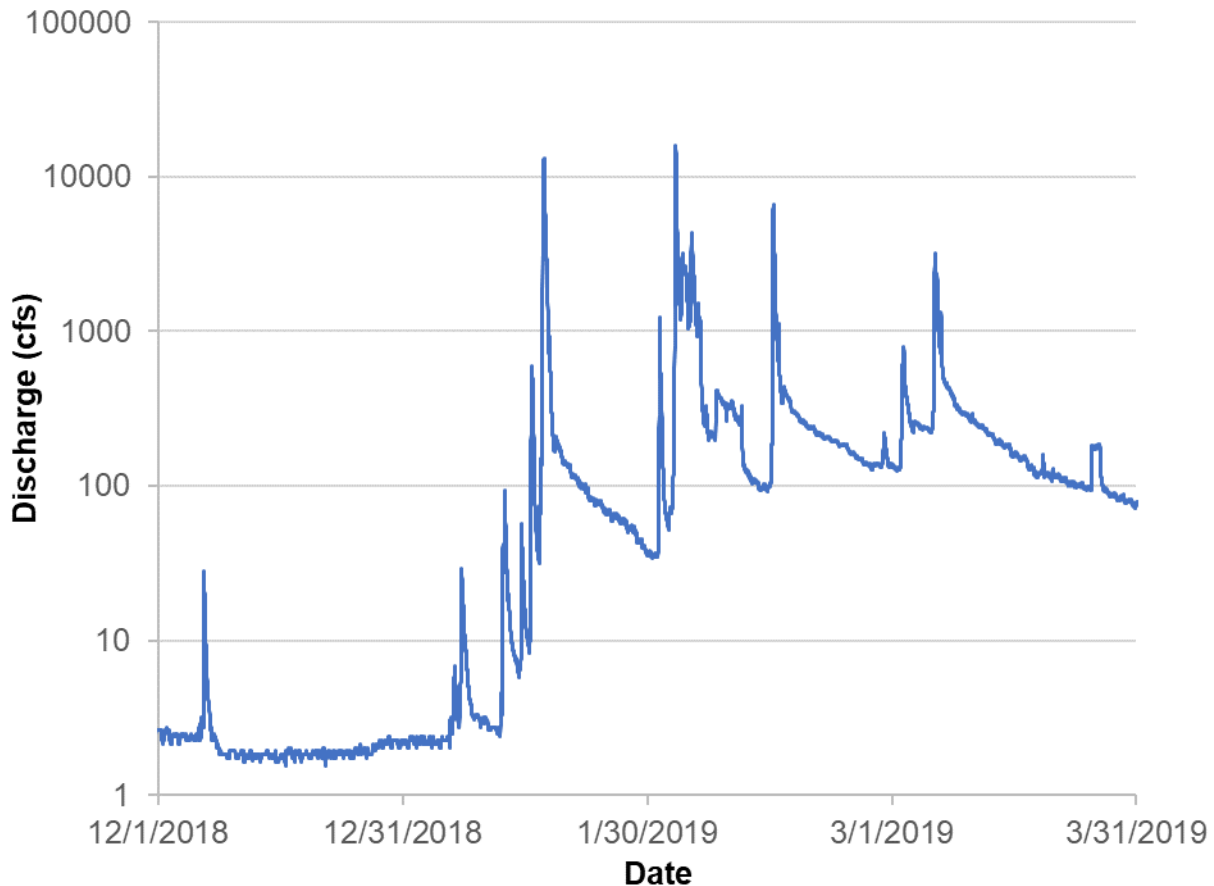


**Figure C-4.** Semi-log-scale of 15-minute flow data from the USGS 11118500, located near Foster Park, from 12/1/2018 to 3/31/2019, showing the major storm events of the 2019 water year.

## C.2 HEC-RAS Model Construction Methods

The basic elements of the HEC-RAS model construction are the same as River2D; a computational mesh is laid over a DTM of the bed topography, and boundary conditions are defined to calibrate flow simulations. The primary difference between the two programs is the relationship between HEC-RAS and geographic information systems (GIS). HEC-RAS requires the DTM be georeferenced, whereas the DTM in River2D can be georeferenced or use a local coordinate system. The DTM was developed in ArcView GIS (ArcView) (ESRI 2011) and imported into HEC-RAS.

The process of developing the DTM in HEC-RAS is similar to River2D. The horizontal location (northing and easting) and bed elevation of all the points collected from the RTK GPS, total station, and LIDAR are combined in a single spreadsheet tab and imported into ArcView GIS as a shape file. The topographic projection of the survey points is defined in the shape file. The shape file is first converted to a triangular

irregular network (TIN), and finally converted to a raster. The raster can be exported from ArcView as a GeoTIFF. The GeoTIFF is imported into HEC-RAS as the DTM, referred to in HEC-RAS as the Terrain layer (Figure C-5). The computational mesh is later defined in HEC-RAS.

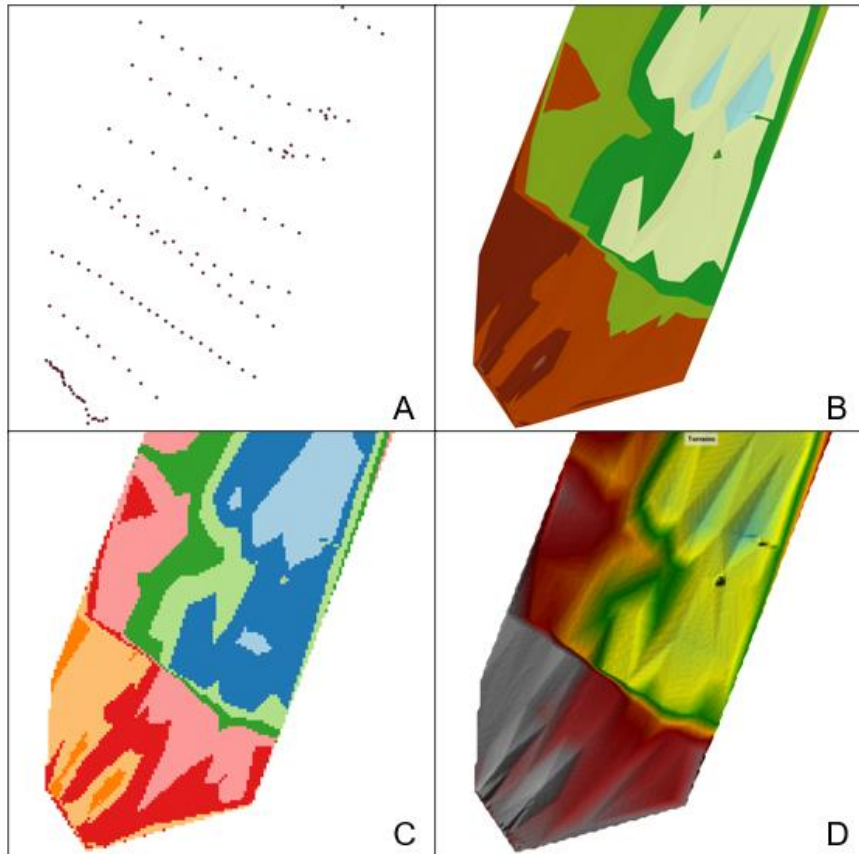


**Figure C-5.** Digital Terrain Model development: (A) bed topography points in ArcView; (B) TIN in ArcView; (C) Raster in ArcView; and (D) Terrain layer in HEC-RAS.

Model development in HEC-RAS starts by defining the 2D Flow Area by drawing a boundary within the outer boundary of the Terrain layer. Next, boundary condition lines are added to the upstream and downstream ends of the 2D Flow Area that define where flow enters and exits the model, respectively. The computational mesh is first defined by adding computational points to the 2D Flow Area on a regular interval. The initial grid is structured with square or rectangular elements with constant mesh cell size and spacing. Cells along the boundary of the 2D Flow Area are a combination of triangles, squares and rectangles to conform to the boundary shape. HEC-RAS can handle unstructured mesh cells with up to 8 faces. If cells are generated with more than 8 faces, the cell boundary is automatically highlighted in red. Red cells can be modified to reduce the number of cell faces to 8 or less by: 1) adjusting the location of the cell center; 2) deleting a cell center; 3) adding a new cell center; or 4) a combination of the three methods.

There is a major difference in the relationship between the DTM and the computational mesh from River2D to HEC-RAS. In HEC-RAS the computational mesh is detached from the DTM; the DTM is converted into a TIN prior to the application of the computational mesh. Cell computations for WSEL are read along each cell face with one single cell centered WSEL. In HEC-RAS, the resolution of change in WSEL is a function of cell size. Depth is different; because the mesh is detached from the DTM, multiple depths can be calculated across the cell face surface based on the underlying terrain, referred to in HEC-RAS as sub-grid bathymetry (Figure C-6).

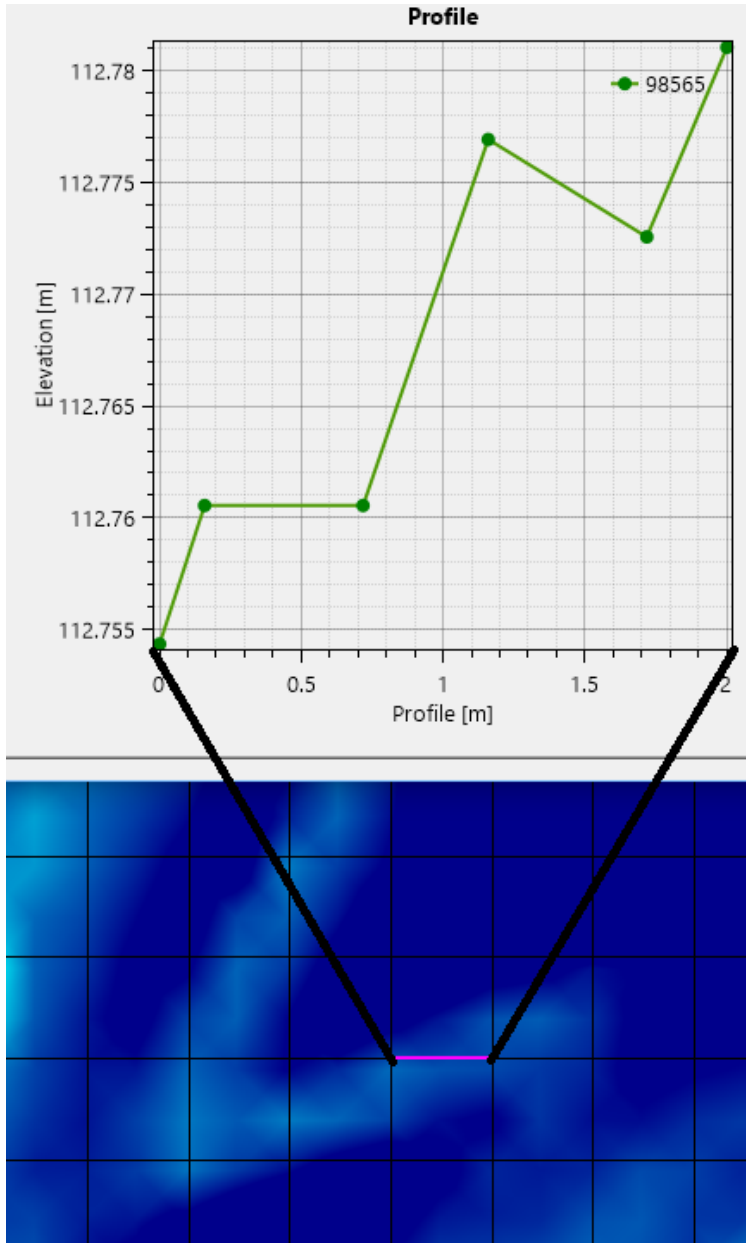


**Figure C-6.** HEC-RAS Sub-grid Bathymetry. The pink grid line is flat, but considers the varied terrain below shown by the elevation profile above the grid. The number 98565 is the reference for the cell face in the model.

Model run times are reduced with larger cell sizes because there are less computations being performed in any given simulation. In a hydraulic system where the WSEL varies gradually, the concept of sub-grid bathymetry allows the user to minimize runs times by using larger cell sizes without losing resolution. In areas where WSEL varies, the required resolution must be controlled by the computational mesh cell size.

The two primary ways to manipulate the computational mesh in HEC-RAS are by adding breaklines and performing region refines of the mesh cell sizes in areas with complex terrain and/or hydraulics. These are the same methods used in River2D, but the application in HEC-RAS is different. In HEC-RAS, breaklines are added in the geometry editor to enforce a feature that is a barrier to flow or controls the direction of flow. Breaklines are used to define ridge lines in the model to prevent flow from leaking across cell faces. Breaklines also prompt the program to add unstructured mesh cells. Region refines are used to reduce the cell spacing, thus increasing the WSEL resolution in a selected area of the computational mesh. Region refines are added in the RAS Mapper utility. The amount of cell size refinement is constrained by the flow velocity across the mesh cell; smaller mesh sizes require smaller computational timesteps.

Stream bed roughness is defined in HEC-RAS using the Manning's  $n$  roughness coefficient ( $n$ ). A single  $n$  value can be assigned to the model in the 2D Flow Area menu or  $n$  can be spatially varied within the model. There are two ways to use spatial variation: 1) the user may manually define regions in the geometry editor; or 2) the user can import a gridded land cover layer through the RAS Mapper utility. Manually defined regions are ideal when the model is used for flood inundation, where flow exceeds the main-stream channel and inundates a floodplain. Land cover layers have a 30-m resolution and are ideal when the roughness of the Terrain model topography is not homogeneous. An example application of roughness by land cover would be a large-scale model used for flood inundation that included a natural stream channel area, overbank floodplain area, and a developed residential or commercial area.

The intermittent reach study site was modeled using a single  $n$  value. The purpose of the study was to evaluate impediments to fish passage. The flows simulated were limited to in-channel levels. Manning's  $n$  is commonly recommended in ranges based on the characteristics of the open channel being evaluated; for natural channels of irregular sections with pools, a range of 0.04 to 0.10 is recommended (Gupta 1995).

### **C.3 HEC-RAS Model Calibration Methods**

As with River2D, once the HEC-RAS model has been constructed, calibration is required to determine that the model is reliably simulating the flow-WSEL relationship determined through the WSEL calibration process, using the WSELs measured in the field. Simulations are performed in HEC-RAS by defining the 2D flow area in the

geometry editor, defining boundary condition parameters in the unsteady flow data menu, and setting the computational parameters in the unsteady flow simulation menu.

Model development is started by digitizing the 2D flow area within the boundary of the raster based DTM. Next, the boundary condition lines are added, and finally the computational grid spacing is defined. A single n-value was assigned to the computational mesh in the geometry editor. The study site boundary conditions consisted of an upstream inflow and downstream outflow. The boundary conditions are defined in the unsteady flow data menu. Although 2D HEC-RAS is an unsteady flow model, a steady state condition was achieved by assigned a single flow value in the Flow Hydrograph menu for the upstream boundary and a single stage value in the Stage Hydrograph menu for the downstream boundary for a long enough period of time to reach equilibrium. The upstream boundary condition line was assigned a constant flow hydrograph equal to the target simulation flow. The downstream boundary condition was set to a constant stage hydrograph, and the corresponding XS-1 WSEL for the flow simulation was input as the constant stage. The model is then calibrated by comparing the results of the XS-2 WSEL at equilibrium with the value from the XS-2 rating relationship.

The slope of the energy grade (EG) line is an input parameter for the Flow Hydrograph boundary condition. An initial EG slope at XS-2 was computed from the Pre-storm model at the same flow level. After the first simulation the EG slope was checked and modified if necessary.

There are two numerical solution equations available in HEC-RAS, diffusion wave approximation (DWA) and full momentum (FM); both require the user to select an appropriate computational time step for the equations to function properly. The Courant Number (CN) is used to measure whether the time step ( $\Delta T$ ) is short enough to capture the change in wave speed ( $V_s$ ) across the mesh cell ( $\Delta X$ ) as follows:

Diffusion Wave Approximation:  $CN = (V_s \times \Delta T) / \Delta X \leq 2$ ; and

Full Momentum:  $CN = (V_s \times \Delta T) / \Delta X \leq 1$ .

The numerical thresholds are suggested for each equation type (WEST Consultants Inc 2017). Practically, the allowable cell size of the mesh is limited by the maximum expected speed of water moving through a cell. DWA has faster run times and is inherently more stable than FM, but DWA is limited in application. DWA is a good choice when the fluid dynamics can be simplified to the assumptions of Manning's equation. DWA is good with gradually varying flows with moderate to steep slopes. DWA does not appropriately simulate flow separations, eddies, or main channel/overbank momentum transfers. FM should be used with highly dynamic flood waves such as flash flood/dam breach, sudden hydraulic expansion or contraction, tidal conditions, wave run-up, super elevation around bends, detailed velocities and stages

at structures, mixed flow regime simulations, and main channel to overbank momentum transfers (WEST Consultants Inc 2017). DWA was used to determine initial n-values, check EG slope, FN, and the amount of run-time necessary to achieve flow equilibrium across the site. Final flow simulations used to determine depth thresholds for fish passage were rerun using FM to confirm the DWA and FM solutions predicted equal depth for fish passage.

Once a simulation is completed, several hydraulic parameters can be displayed in the RAS-Mapper for each computational mesh cell. Both CN and FN are selection options. After each simulation, the results for both are parameters are reviewed. Depending upon whether the simulation was solved using DWA or FM, values are checked to see if the CN exceeded either 2.0 for DWA or 1.0 for FM. The RAS-Mapper visual display color scale can easily be set to a threshold value to facilitate output data verification. FN is a dimensionless parameter that describes the relationship between water velocity and wave speed. When FN reaches 1.0, the water velocity exceeds the wave speed, and upstream traveling waves are washed downstream (Munson et al. 1998). At FN equals 1.0, flow transitions from laminar subcritical flow to critical flow and as FN becomes greater than 1.0 to supercritical flow. Supercritical conditions are characterized by turbulent flow, the onset of vertical mixing, a break in hydraulic slope continuity, or a hydraulic jump (Munson et al. 1998). Although HEC-RAS is capable of solving water depth in critical to supercritical flow conditions, depths estimated from a 2D model in subcritical, ideally laminar flow, are less variable.

#### **C.4 HEC-RAS Depth Validation Methods**

Depth validation is the final step after the 2D model is calibrated and simulations have been completed over the flow range required for the passage evaluation. Water depths are measured at random locations within the study site. The exact location and stream bed elevation are recorded with RTK GPS. A discharge measurement is taken before the validation depth measurements are recorded. A 2D model simulation is completed at the flow recorded in the field. The field depth measurements are compared to the depths predicted by the 2D model at the same locations and at the same flow level.

## C.5 HEC-RAS Flow-WSEL Calibration Results

The discharges and accompanying WSELs were measured at XS-2 (Table C-1) to develop a flow-water level rating relationship (Figure C-7) for the Post-storm 2D model. The rating data was collected at XS-2 after it was discovered that the PT at XS-2 could not be recovered.

**Table C-1.** XS-2 Discharge-WSEL Log-Log regression data.

Date	Discharge (cfs)	WSEL (ft) (SZF = 389.61)	LOG(Discharge)	LOG(WSEL-SZF)
5/1/2018	2.0	390.24	0.30	-0.20
1/22/2019	53.5	391.13	1.73	0.18
1/23/2019	51.9	391.11	1.72	0.18
1/30/2019	23.0	390.77	1.36	0.06

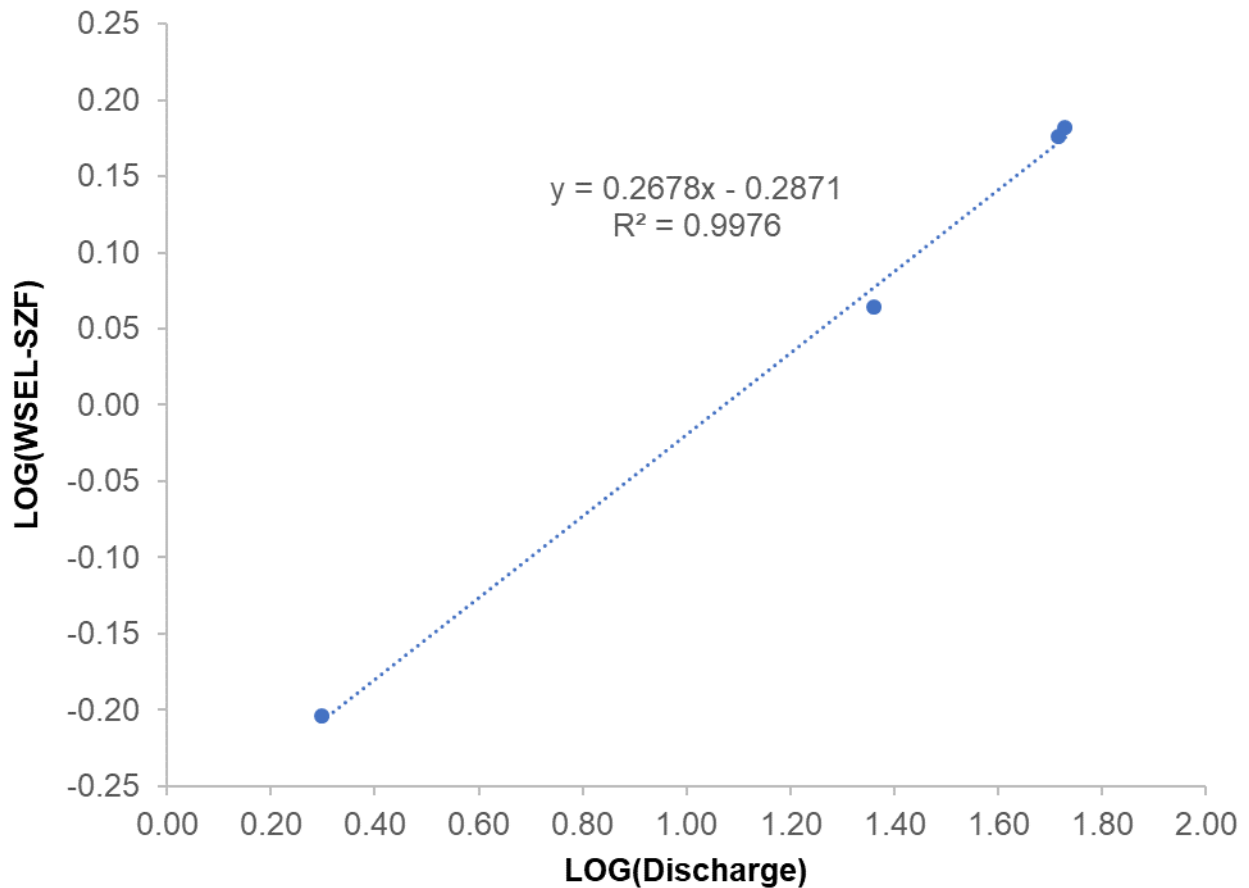


**Figure C-7.** XS-2 Log-Log linear regression.

The discharges measured in the field at XS-2 were compared to the 15-minute flow data reported by USGS at the Foster Park stream gage downstream (Table C-2). The percentage of Foster Park stream gage flow contributed by XS-2 was computed in the last column of Table C-2.

**Table C-2.** Discharge recorded near XS-2 compared to 15-minute flow data published for USGS 11118500.

Date	Time	Discharge XS-2 (cfs)	Flow at Foster Park (cfs)	Percent X-2 of Foster Park (%)
3/27/2018 <sup>h</sup>	09:12-09:55	31.0	46.8	66%
5/1/2018	08:28-10:04	2.0	2.5	79%
1/22/2019	16:19-17:01	53.5	81.4	66%
1/23/2019	08:14-08:57	51.9	71.2	73%
1/30/2019	13:32-14:29	23.0	33.1	69%

The two highest flows recorded, 53.5 cfs and 51.9 cfs, were averaged together to estimate the ratio of flow in the study area versus Foster Park. The flow in the study site was assumed to be 69% of the flow reported by USGS for Foster Park. This ratio was used to relate the flow-WSEL rating for XS-1 to the study site.

The flow-WSEL rating relationship for XS-1 was developed using the same LOG-LOG regression techniques used for the Pre-storm model (Appendix B). The data used to create the rating were from the last descending hydrograph limb prior to the 2018 LIDAR flight. As indicated in the methods section the USGS flows and PT water levels had to be adjusted by a half an hour to account for the lag in the travel time between the site and the USGS stream gage at Foster Park. The USGS flows were converted to study site flows using the 69% factor described above. The PT water levels were converted to WSELs by adding the water levels to the surveyed bed elevation of the PT. The SZF bed elevation, surveyed downstream of XS-1, was subtracted from the WSELs and then plotted versus the study site flows using the LOG-LOG techniques described in Appendix B for the Pre-storm model (Figure C-8). The data used to develop the XS-1 rating are provided in Table C-3.

---

<sup>h</sup> The discharge measurement on 3/27/2018 does not appear in Table C-1 because a corresponding water surface elevation was not recorded for that discharge.

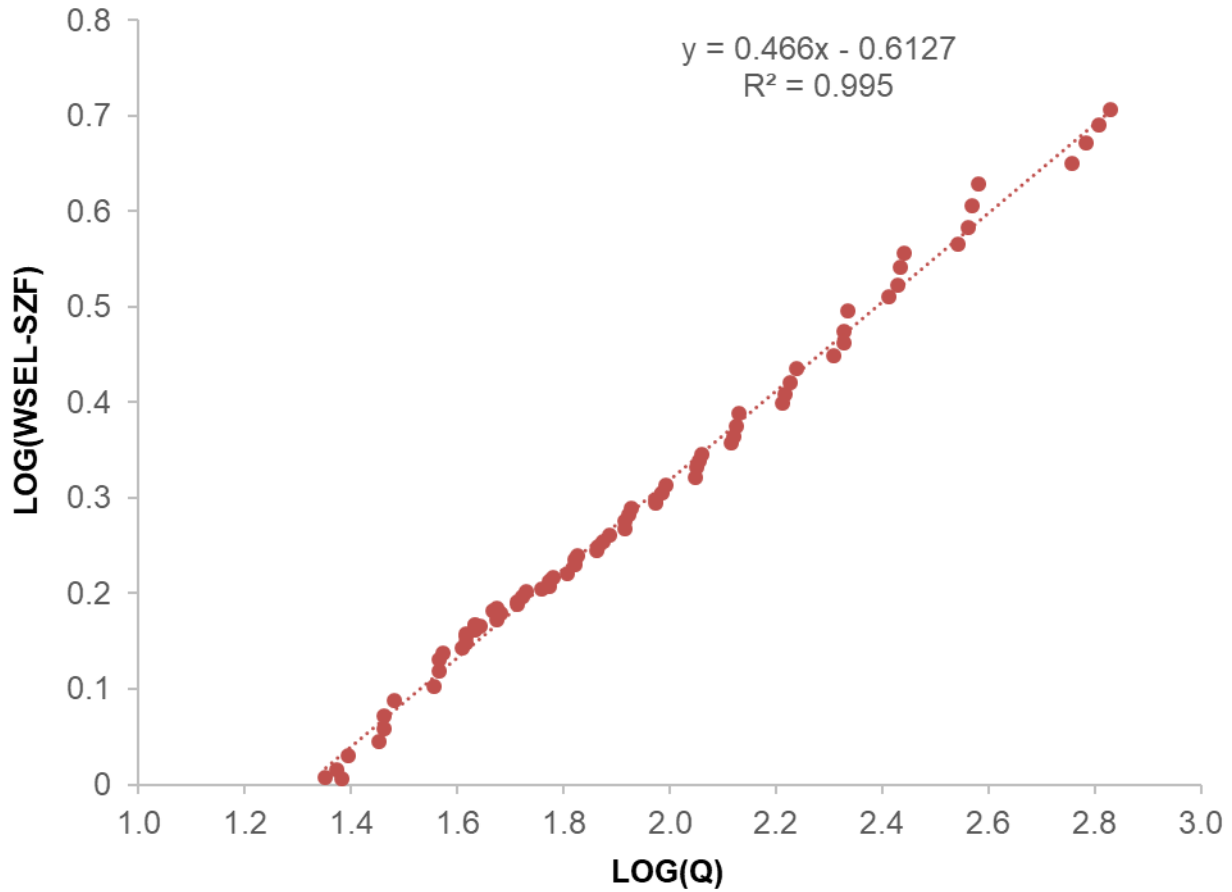


**Figure C-8.** Best-fit flow-WSEL rating relationship for XS-1.

**Table C-3.** Data used to develop the XS-1 flow-WSEL rating relationship.

Date	Time	Flow (cfs)	WSEL (ft)	LOG (Q)	LOG (WSEL-SZF)	Predicted LOG (WSEL-SZF)	Predicted WSEL (ft)	Error
1/9/2018	17:00	673.6	314.59	2.83	0.71	0.71	314.57	-0.02
1/9/2018	17:15	642.4	314.40	2.81	0.69	0.70	314.46	0.06
1/9/2018	17:30	608.4	314.20	2.78	0.67	0.68	314.34	0.14
1/9/2018	17:45	573.1	313.97	2.76	0.65	0.67	314.21	0.24
1/9/2018	18:00	381.8	313.76	2.58	0.63	0.59	313.40	-0.36
1/9/2018	18:15	371.4	313.54	2.57	0.61	0.58	313.35	-0.19
1/9/2018	18:30	363.8	313.34	2.56	0.58	0.58	313.31	-0.03
1/9/2018	18:45	349.2	313.18	2.54	0.57	0.57	313.24	0.05
1/9/2018	19:00	276.5	313.10	2.44	0.56	0.53	312.85	-0.25
1/9/2018	19:15	272.3	312.98	2.44	0.54	0.52	312.83	-0.15
1/9/2018	19:30	268.2	312.83	2.43	0.52	0.52	312.80	-0.03
1/9/2018	19:45	259.2	312.74	2.41	0.51	0.51	312.75	0.01

Date	Time	Flow (cfs)	WSEL (ft)	LOG (Q)	LOG (WSEL-SZF)	Predicted LOG (WSEL-SZF)	Predicted WSEL (ft)	Error
1/9/2018	20:00	216.9	312.63	2.34	0.50	0.48	312.49	-0.14
1/9/2018	20:15	213.4	312.49	2.33	0.48	0.47	312.47	-0.02
1/9/2018	20:30	213.4	312.40	2.33	0.46	0.47	312.47	0.07
1/9/2018	20:45	203.7	312.31	2.31	0.45	0.46	312.41	0.09
1/9/2018	21:00	173.2	312.22	2.24	0.43	0.43	312.20	-0.03
1/9/2018	21:15	168.4	312.14	2.23	0.42	0.42	312.16	0.02
1/9/2018	21:30	164.9	312.06	2.22	0.41	0.42	312.13	0.07
1/9/2018	21:45	163.5	312.01	2.21	0.40	0.42	312.12	0.12
1/9/2018	22:00	135.1	311.94	2.13	0.39	0.38	311.90	-0.04
1/9/2018	22:15	133.7	311.88	2.13	0.38	0.38	311.89	0.01
1/9/2018	22:30	132.4	311.82	2.12	0.36	0.38	311.88	0.06
1/9/2018	22:45	131.0	311.78	2.12	0.36	0.37	311.87	0.09
1/9/2018	23:00	115.0	311.72	2.06	0.35	0.35	311.73	0.01
1/9/2018	23:15	113.6	311.68	2.06	0.34	0.35	311.71	0.03
1/9/2018	23:30	112.3	311.65	2.05	0.33	0.34	311.70	0.06
1/9/2018	23:45	111.6	311.60	2.05	0.32	0.34	311.70	0.10
1/10/2018	0:00	98.4	311.56	1.99	0.31	0.32	311.57	0.01
1/10/2018	0:15	97.0	311.52	1.99	0.31	0.31	311.56	0.04
1/10/2018	0:30	94.2	311.49	1.97	0.30	0.31	311.53	0.04
1/10/2018	0:45	94.2	311.47	1.97	0.29	0.31	311.53	0.06
1/10/2018	1:00	84.5	311.44	1.93	0.29	0.29	311.43	-0.01
1/10/2018	1:15	83.8	311.42	1.92	0.28	0.28	311.42	0.01
1/10/2018	1:30	82.5	311.39	1.92	0.28	0.28	311.41	0.02
1/10/2018	1:45	82.5	311.36	1.92	0.27	0.28	311.41	0.05
1/10/2018	2:00	76.9	311.32	1.89	0.26	0.27	311.35	0.02
1/10/2018	2:15	74.8	311.30	1.87	0.25	0.26	311.32	0.03
1/10/2018	2:30	73.5	311.27	1.87	0.25	0.26	311.31	0.03
1/10/2018	2:45	72.8	311.26	1.86	0.24	0.25	311.30	0.04
1/10/2018	3:00	67.3	311.24	1.83	0.24	0.24	311.24	0.00
1/10/2018	3:15	66.3	311.22	1.82	0.24	0.24	311.22	0.00
1/10/2018	3:30	66.3	311.20	1.82	0.23	0.24	311.22	0.02
1/10/2018	3:45	64.2	311.16	1.81	0.22	0.23	311.20	0.03
1/10/2018	4:00	60.3	311.15	1.78	0.22	0.22	311.15	0.00
1/10/2018	4:15	59.3	311.13	1.77	0.21	0.21	311.14	0.00
1/10/2018	4:30	59.3	311.12	1.77	0.21	0.21	311.14	0.02
1/10/2018	4:45	57.4	311.10	1.76	0.20	0.21	311.11	0.01
1/10/2018	5:00	53.6	311.09	1.73	0.20	0.19	311.06	-0.03
1/10/2018	5:15	52.7	311.07	1.72	0.20	0.19	311.05	-0.02

Date	Time	Flow (cfs)	WSEL (ft)	LOG (Q)	LOG (WSEL-SZF)	Predicted LOG (WSEL-SZF)	Predicted WSEL (ft)	Error
1/10/2018	5:30	51.8	311.06	1.71	0.19	0.19	311.04	-0.02
1/10/2018	5:45	51.8	311.04	1.71	0.19	0.19	311.04	-0.01
1/10/2018	6:00	47.4	311.03	1.68	0.19	0.17	310.97	-0.06
1/10/2018	6:15	46.6	311.02	1.67	0.18	0.16	310.96	-0.06
1/10/2018	6:30	48.2	311.01	1.68	0.18	0.17	310.99	-0.02
1/10/2018	6:45	47.4	310.99	1.68	0.17	0.17	310.97	-0.01
1/10/2018	7:00	43.2	310.97	1.64	0.17	0.15	310.91	-0.06
1/10/2018	7:15	43.2	310.97	1.64	0.17	0.15	310.91	-0.06
1/10/2018	7:30	44.0	310.97	1.64	0.17	0.15	310.92	-0.04
1/10/2018	7:45	43.2	310.95	1.64	0.16	0.15	310.91	-0.04
1/10/2018	8:00	41.5	310.94	1.62	0.16	0.14	310.89	-0.06
1/10/2018	8:15	41.5	310.93	1.62	0.16	0.14	310.89	-0.04
1/10/2018	8:30	41.5	310.91	1.62	0.15	0.14	310.89	-0.02
1/10/2018	8:45	40.7	310.89	1.61	0.14	0.14	310.87	-0.02
1/10/2018	9:00	37.6	310.87	1.57	0.14	0.12	310.82	-0.05
1/10/2018	9:15	36.8	310.85	1.57	0.13	0.12	310.81	-0.04
1/10/2018	9:30	36.8	310.82	1.57	0.12	0.12	310.81	-0.01
1/10/2018	9:45	36.0	310.77	1.56	0.10	0.11	310.80	0.03
1/10/2018	10:00	30.4	310.72	1.48	0.09	0.08	310.70	-0.02
1/10/2018	10:15	29.1	310.68	1.46	0.07	0.07	310.67	-0.01
1/10/2018	10:30	29.1	310.64	1.46	0.06	0.07	310.67	0.03
1/10/2018	10:45	28.4	310.61	1.45	0.04	0.06	310.66	0.05
1/10/2018	11:00	24.8	310.57	1.39	0.03	0.04	310.59	0.02
1/10/2018	11:15	23.7	310.54	1.37	0.02	0.03	310.57	0.03
1/10/2018	11:30	24.2	310.52	1.38	0.01	0.03	310.58	0.06
1/10/2018	11:45	22.5	310.52	1.35	0.01	0.02	310.54	0.02

The flow-WSEL ratings developed for XS-1 were used as the boundary conditions to perform the flow simulations in HEC-RAS to estimate depth and width of water for fish passage, while the flow-WSEL ratings developed for XS-2 were used to calibrate the HEC-RAS model.

## C.6 HEC-RAS Model Construction Results

Before the 2018 LIDAR data became available, the Post-storm DTM was constructed using topographic survey points collected post storm in the same manner as the Pre-storm model. The 2005 LIDAR data was used in the same manner as the Pre-storm

model to fill in primarily overbank areas, steep banks, and cliff faces that could not be safely surveyed, and private property areas within the floodplain. The Post-storm field survey points and 2005 LIDAR data collected were organized in ArcView. The River2D utility program BED\_R2D was used to identify erroneous points in the bed topography.

A total of 26,379 of 26,407 points were used to create the field survey based DTM; 5 points were deleted because they were duplicates of existing points, and 23 points were deleted because there had erroneous elevations that could not be corrected. The total number of LIDAR points adjacent to field surveyed points was approximately 2,800. A total of 116 LIDAR points were deleted because their elevations were erroneous when compared with the survey points located near them.

The Post-storm model field survey and LIDAR points were first converted into a TIN surface, then converted to a raster. The raster conversion was performed using the linear method and the Cell Size was set to 1 m. The Linear method is the recommended default in ArcView. A 1-m cell size was selected to allow a 1-m grid size in HEC-RAS if necessary. The Post-storm raster was saved as a GeoTIFF and imported into the HEC-RAS. The imported GeoTIFF is the basis for the georeferenced DTM and termed Terrain layer in HEC-RAS.

Once the 2018 LIDAR data became available, the existing Post-storm DTM was compared with the 0.25-m LIDAR. The most important areas to compare were the locations of passage-limiting riffles where the resolution of the DTM would have the most bearing on evaluating depth for fish passage. The location of riffle number 20 (R20) from the critical rifle survey is shown in Figure 17 in the Technical Report. The DTM developed from the field survey data and the 2005 LIDAR is compared to the 2018 LIDAR at Riffle 20 in Figure C-9. The resolution of the 2018 LIDAR data is superior. The 2018 LIDAR was used instead of the original DTM to evaluate water depth and width for fish passage.

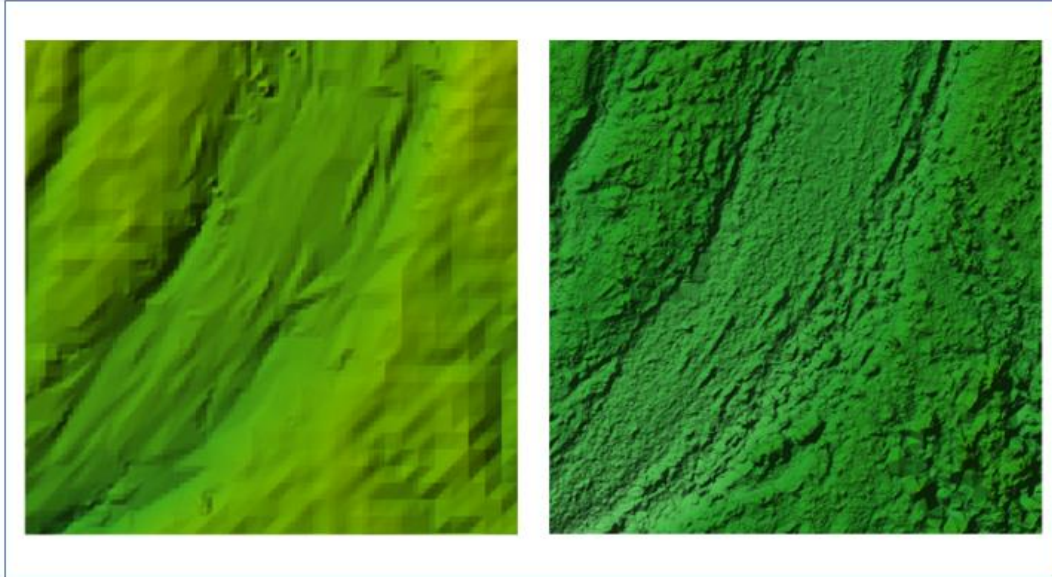


**Figure C-9.** DTM generated from field survey points and 2005 3-m LIDAR (left) compared to 2018 0.25-m QL1 LIDAR (right).

The 2018 LIDAR-based DTM had to be improved to replace the original DTM. The original in-channel field survey had the advantage of gathering ground elevations in areas with standing water, like pools, where LIDAR is less likely to penetrate. Fortunately, the 2018 flight was performed when the water level in the river was low, at approximately 3 cfs. Even at 3 cfs, there were large areas where the ground surface elevations were obscured by standing water. To improve the DTM, the areas of the LIDAR DTM containing the largest pooled areas were replaced with data from the field based topographic survey data. Four large areas where standing water obscured the 2018 LIDAR flight were replaced with the original field survey points.

The four survey point grafts were prepared and are identifiable by white boundaries in Figure C-10. Cross section A-A' in Figure C-10 was cut across one of the grafted areas. Figure C-11 shows the area before and after the graft, and the cross section profiles of the bed elevations. The red-dotted line is the original 2018 LIDAR and the solid blue line is the actual field-based survey data. The field-based survey data captured the depth and extent of the pool structure.

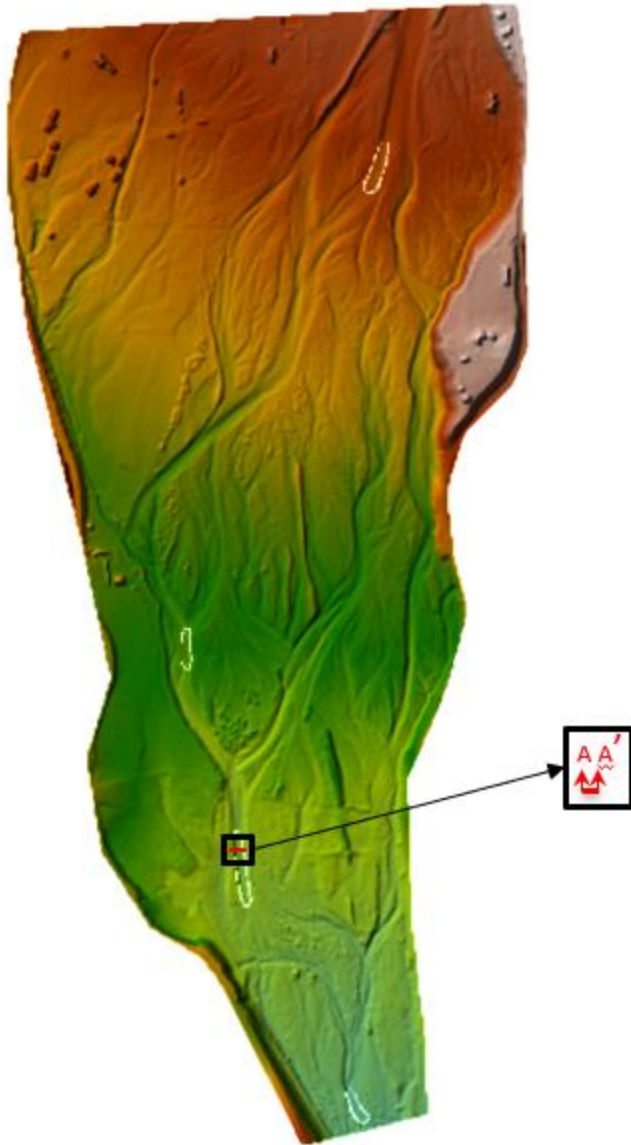
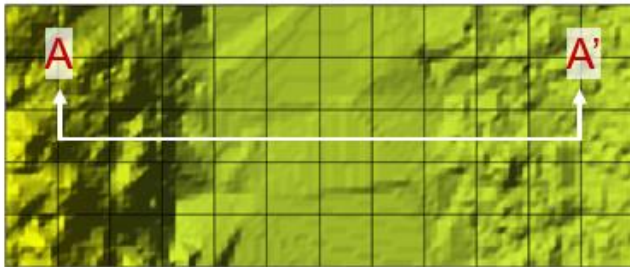


**Figure C-10.** DTM using 2018 LIDAR and field survey points located in areas where the ground surface was obscured by standing water, survey point areas are marked by white lines.

DTM before field survey graft



DTM after field survey graft

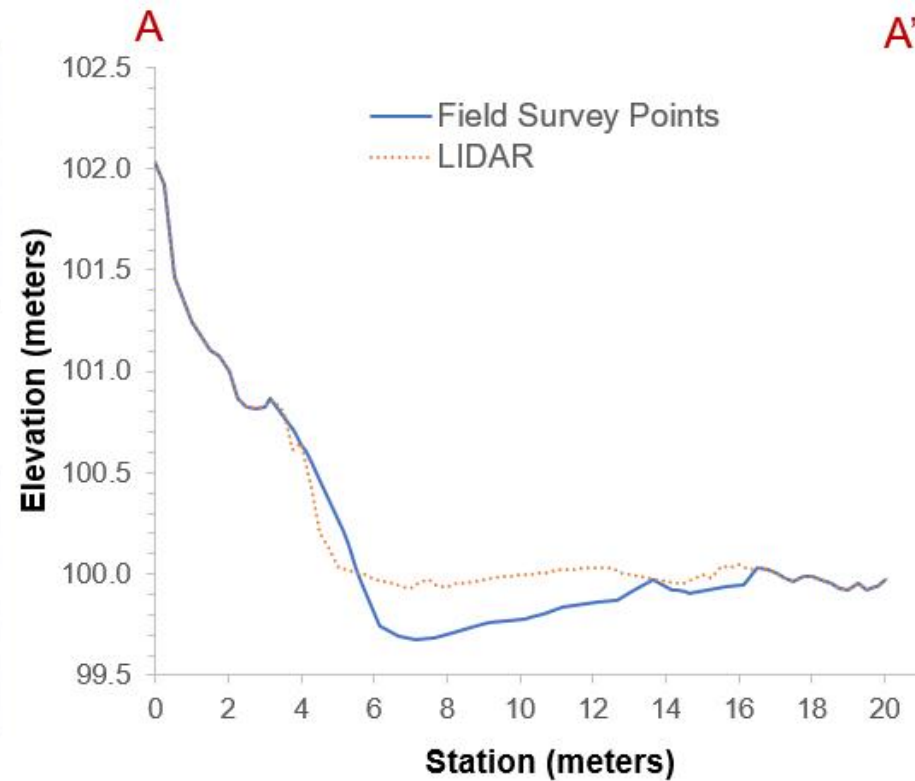
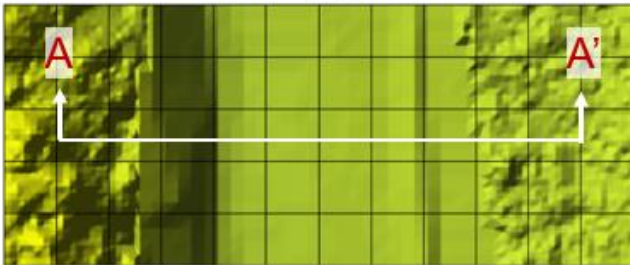


**Figure C-11.** Left side images are the in-channel bed at cross section A-A' before and after the 2018 LIDAR GeoTIFF was replaced with the survey point data. On the right is the bed elevation profile of the cross sections. The red-dotted line is the original 2018 LIDAR bed elevation profile and the solid blue line is the bed elevation profile along the cross section.

The HEC-RAS Mapper utility accepts multiple GeoTIFFs and stitches layers one on top another into a single composite GeoTIFF. GeoTIFFs of the four large pool areas using the data points from the field survey were created in ArcView and imported into HEC-RAS. The pool area GeoTIFFs, with a 0.5-m cell size, were then layered over the 2018 LIDAR, with a 0.25-m cell size, in the HEC-RAS Mapper utility. The composite GeoTIFF was opened in the geometric editor utility of HEC-RAS and a 2D Flow Area was established by drawing the external boundary just inside the limits of the Terrain layer. Next, computational points were generated on a regular 2-m interval (Figure C-6). The Boundary Condition lines were added to the upstream and downstream ends of the model where flow enters upstream and exits downstream.

## **C.7 HEC-RAS Model Calibration Results**

The HEC-RAS model was used to predict water depths within the study site and evaluate passage conditions for adult steelhead over a range of flows. Flow simulations were initially run at 100 cfs and 50 cfs to screen for the most critical riffles (Table C-3). Next, flows were simulated at 400 cfs, 300 cfs, 200 cfs, and 150 cfs to determine the range where flows would meet the passage criteria. Additional simulations were performed at increments of 50 cfs, 10 cfs, and finally 5 cfs to target flows meeting the passage criteria of 10 contiguous feet (Table C-4). The WSEL at XS-1 was held constant during the simulation using the stage hydrograph boundary condition. A constant flow was set at the upstream boundary using the flow hydrograph boundary condition. Each flow simulation was run until flow equilibrium was reached at the upstream and downstream model boundaries. The flow simulations were calibrated by comparing the WSEL at XS-2, at equilibrium, with the WSEL from the XS-2 rating relationship (Table C-4).

**Table C-4.** Flow-WSEL rating relationships used to calibrate HEC-RAS Post-storm model, WSELs adjusted to 2018 LIDAR.

Site Discharge (cfs)	XS-1 WSEL (ft)	XS-2 WSEL (ft)	Site Discharge (cms)	XS-1 WSEL (m)	XS-2 WSEL (m)
400	313.48	392.18	11.327	95.549	119.537
300	312.98	391.99	8.495	95.397	119.479
200	312.38	391.75	5.663	95.214	119.405
150	312.02	391.59	4.248	95.104	119.356
145	311.98	391.57	4.106	95.092	119.351
140	311.94	391.55	3.964	95.080	119.345
135	311.90	391.53	3.823	95.067	119.340
130	311.86	391.52	3.681	95.054	119.334
125	311.82	391.50	3.540	95.041	119.328
120	311.77	391.47	3.398	95.028	119.322
105	311.63	391.41	2.973	94.986	119.302
100	311.59	391.39	2.832	94.972	119.294
50	311.01	391.09	1.416	94.796	119.203
17	310.46	390.72	0.481	94.629	119.090

The model run times were set to achieve flow equilibrium within the site and at the downstream boundary cross section. Flow simulations were calibrated until the WSEL simulated at XS-2 was within the required tolerance of 0.1 ft (USFWS 2011) compared with the predicted WSEL by the Post-storm model rating relationship (Table C-5). An initial Manning’s n roughness coefficient of 0.075 was used at 400 cfs to calibrate the model. As Manning’s n varies with discharge (Chow 1959), Manning’s n increased steadily as WSEL receded with decreasing flow levels, and the influence of the bed roughness at XS-2 increased (Figure C-12).

**Table C-5.** Post-storm HEC-RAS model Manning's n and WSEL/flow simulation results using DWA for all flows and FM at selected flows.

<b>Flow (cfs)</b>	<b>Solution type</b>	<b>Manning's n</b>	<b>Rating at XS-2 WSEL (ft)</b>	<b>HEC-RAS XS-2 WSEL (ft)</b>	<b>(+/-) (ft)</b>
400	DWA	0.075	392.18	392.14	-0.04
300	DWA	0.085	391.99	391.98	-0.01
200	DWA	0.095	391.75	391.74	-0.01
150	DWA	0.105	391.59	391.59	0.00
145	DWA	0.105	391.57	391.57	0.00
145	FM	0.105	391.57	391.56	-0.01
140	DWA	0.105	391.55	391.54	-0.01
135	DWA	0.105	391.53	391.52	-0.01
130	DWA	0.105	391.52	391.49	-0.03
125	DWA	0.105	391.50	391.46	-0.04
120	DWA	0.105	391.47	391.43	-0.04
105	DWA	0.105	391.41	391.35	-0.06
100	DWA	0.105	391.39	391.32	-0.07
100	FM	0.105	391.39	391.32	-0.07
50	DWA	0.13	391.09	391.05	-0.04
50	FM	0.13	391.09	391.05	-0.04
17	DWA	0.15	390.72	390.66	-0.06
17	FM	0.15	390.72	390.66	-0.06

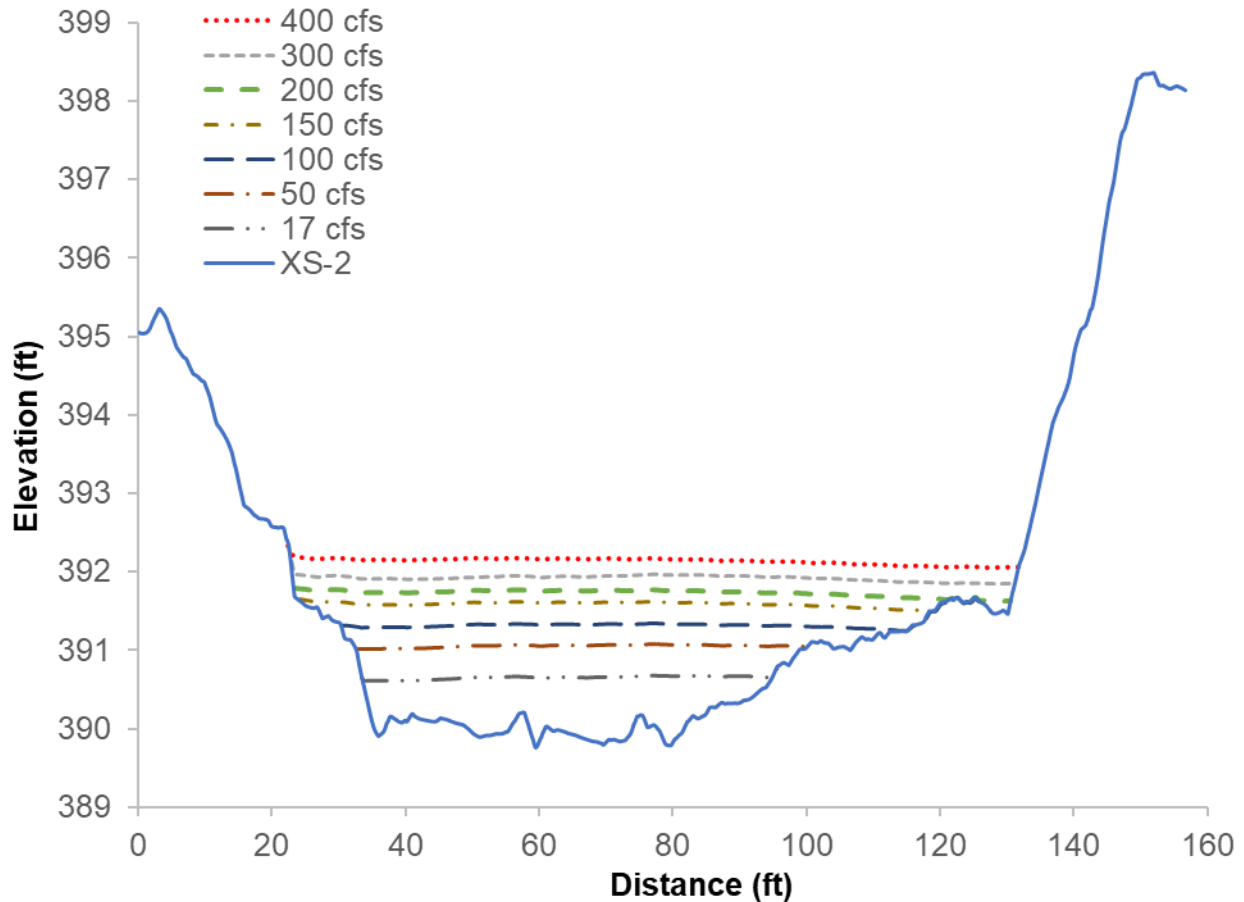


**Figure C-12.** Flow-WSEL results at XS-2 from HEC-RAS.

The results of the DWA and FM solutions were consistent with each other. There was a difference of 0.01 ft between the simulated average WSEL at XS-2 for 145 cfs. The simulation at 145 cfs was key in selecting the critical flow need for fish passage. To ensure there was no difference in the simulations prediction of depth for passage, the contiguous width at Riffle 8 was computed for both and found to be the same (i.e., 10.44 ft) for each solution.

Bed roughness is not the only parameter that must be set in HEC-RAS to execute a simulation. When using a Flow Hydrograph as the upstream boundary condition, the EG slope must be estimated. The WSEL slope was measured at the upstream end of the River2D model at the HEC-RAS first simulation flow of 400 cfs. Once the first HEC-RAS simulation had been completed, an iterative approach was used. The EG slope was recomputed after each simulation and adjusted where necessary. EG slope ranged from 0.012 ft/ft at 400 cfs to 0.005 ft/ft at 17 cfs.

The results in Table C-5 indicated acceptable calibration for the eight flow simulations used to estimate depth for passage and included the validation depth flow simulation at

17 cfs, based on the WSEL predicted at XS-2. The WSELs predicted at XS-2 were all within the 0.1-ft threshold suggested for flow-WSEL calibration (USFWS 2011).

After WSEL calibration was completed for each simulation, the remaining simulation threshold parameters were generated (Table C-6). Net Q refers to the difference between the value of the constant flow hydrograph defined at the upstream boundary and the final value of the flow output hydrograph reported for the downstream boundary at the end of the simulation. CN and FN are field variable options in HEC-RAS and were exported to ArcView as Tiffs for each flow simulation and computational mesh cell. The Tiff layers were classified in ArcView which computes multiple statistics, including average and maximum.

**Table C-6.** Post-storm HEC-RAS model parameters using DWA for all flows and FM at selected flows.

Flow (cfs)	Solution	Final Simulation Flow (cfs)	Net Q	Maximum CN	Average FN	Maximum FN
400	DWA	400.00	0.00%	1.52	0.36	11.11
300	DWA	300.00	0.00%	1.28	0.31	8.98
200	DWA	200.00	0.00%	1.02	0.27	9.22
150	DWA	150.00	0.00%	0.91	0.24	6.61
145	DWA	145.00	0.00%	0.90	0.24	7.41
145	FM	145.00	0.00%	0.90	0.23	6.15
140	DWA	140.00	0.00%	1.78	0.24	7.02
135	DWA	135.00	0.00%	1.76	0.23	7.72
130	DWA	130.00	0.00%	1.75	0.23	6.51
125	DWA	125.00	0.00%	1.73	0.23	7.40
120	DWA	119.96	0.03%	1.71	0.23	6.20
105	DWA	105.00	0.00%	1.65	0.22	6.83
100	DWA	100.00	0.00%	1.63	0.23	6.14
100	FM	100.00	0.00%	0.41	0.22	7.66
50	DWA	50.00	0.00%	0.85	0.17	4.75
50	FM	50.00	0.00%	0.81	0.17	4.99
17	DWA	17.00	0.00%	0.60	0.13	4.02
17	FM	17.00	0.00%	0.20	0.12	4.44

The Net Q for the simulations used to estimate fish passage were below the suggested threshold of 1% (Steffler and Blackburn 2002). The CN values for each computational mesh cell solved using DWA were below the threshold of 2.0 and for mesh cells solved using FM were below the recommended threshold of 1.0. FN was evaluated in each simulation; the maximum FN for an individual cell exceeded 1.0 in all the simulations. FN values were below 1.0 in the flow areas of the main channel, including the critical riffle areas evaluated for fish passage. Computational mesh cells with FNs >1.0 were only observed around the perimeters of substrates protruding above the water surface and sporadically along the wetted stream margins (Figure C-13).

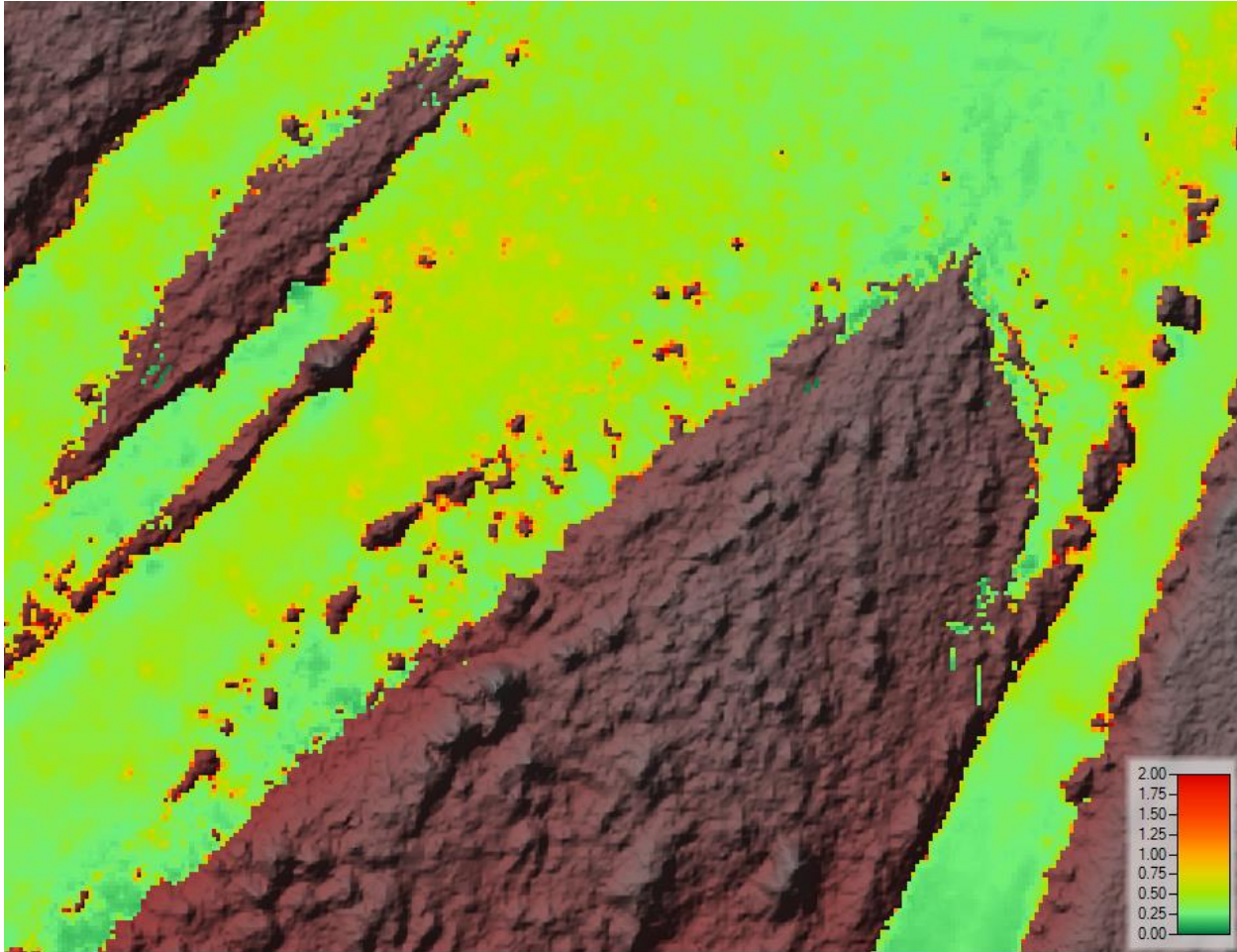


**Figure C-13.** Froude number display at 300 cfs at R23. Only red and orange cells near bed, bank, and substrate boundaries exceed 1.0.

### C.8 HEC-RAS Depth Validation Results

Depth validation measurements were recorded on April 5, 2017 for the Post-storm 2D model. During the data collection process, water depths were measured at 50 random locations within the study site for model validation (Figure C-14). A discharge of 17 cfs was measured near the downstream boundary of the study site before the validation depths were recorded. Each water depth validation location and bed elevation was recorded using an RTK-GPS, and the water depth was measured using a stadia rod. The depth validation points were collected near the downstream boundary of the site.



**Figure C-14.** Post-storm model depth validation locations overlain on 2018 QL1 LIDAR DTM at a simulated flow level of 17 cfs (distances in meters).

The black dots in Figure C-14 represent the locations of the depth validation measurements. The magenta and black colored lines are artifacts produced by the profile line function of the HEC-RAS program. The numbers in the white boxes within Figure C-14 are an indicator of distance on a regular interval and are an artifact of the HEC-RAS profile line function. The validation depths measured in the field were plotted against the depths predicted by HEC-RAS at 17 cfs (Figure C-15) for both DWA and FM solutions. The predicted depths did not correlate well with the depths measured in the field, as indicated by the low  $R^2$  values for both solutions. The cause of the variance is likely because the field validation depths were measured in April 2017, while the 2018 LIDAR used to generate the DTM was flown in late January to early February of 2018. In between those two time periods, a large storm occurred in January 2018 (Figures C-1 and C-2) with a peak flow of over 6,000 cfs. The magnitude of the January 2018 storm exceeded the channel forming flow threshold of 1,876 cfs, and likely led to changes in the stream bed geometry. Changes in the bed elevations of the river where the

validation depths were measured is the most likely cause of the variance in measured versus predicted water depths.

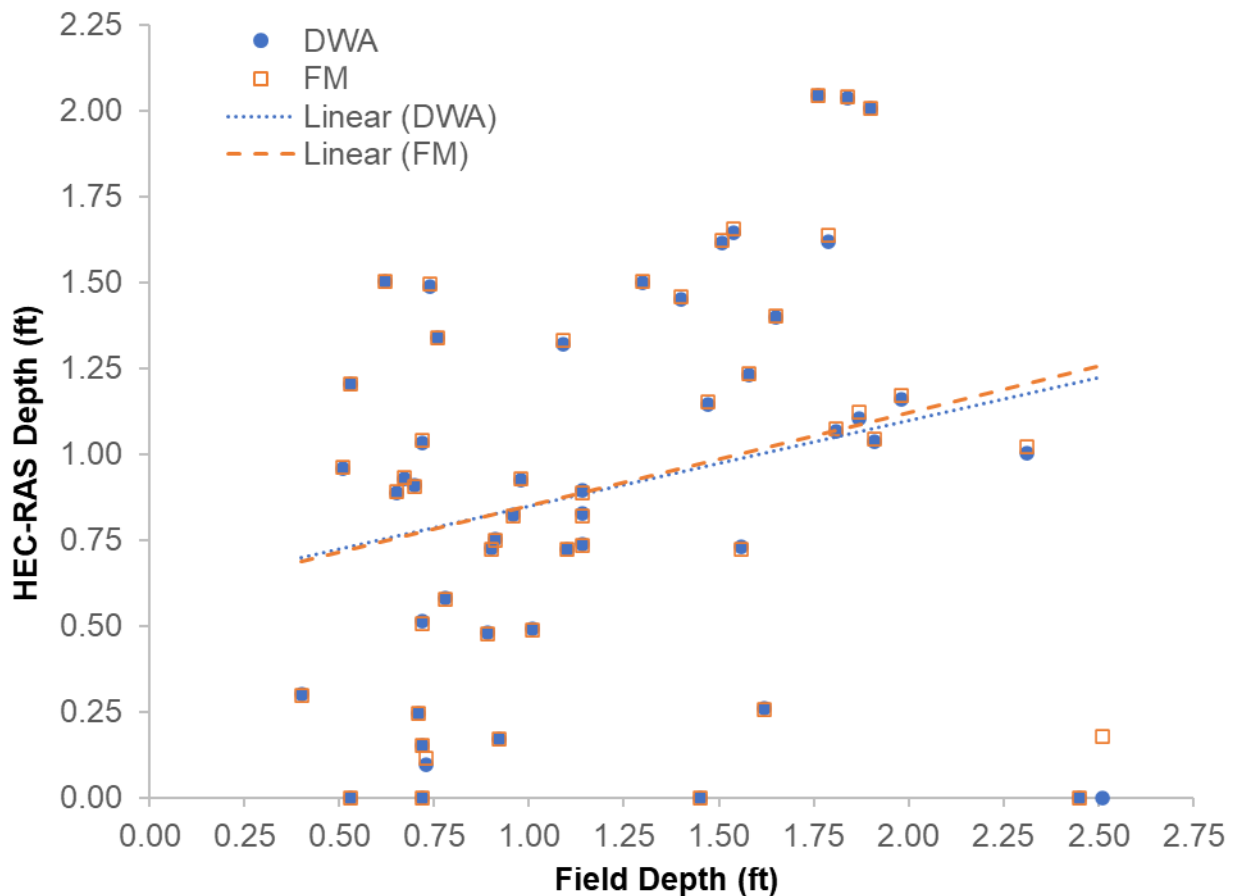


**Figure C-15.** Plot of validation depths at 17 cfs collected in the field with the corresponding predicted depths from HEC-RAS using the DWA and FM solutions. The correlation coefficient ( $R^2$ ) was 0.0592 for the DWA solution and 0.0696 for the FM solution.

WSELs were computed by adding the depth to the bed elevation recorded at each validation depth field survey point. The field derived WSELs were plotted versus the WSELs predicted by the HEC-RAS model at 17 cfs (Figure C-16). The results indicate a correlation between the water surface gradient measured in the field and the model results at 17 cfs in the lower portion of the site where the validation depths were recorded (Figure C-14).

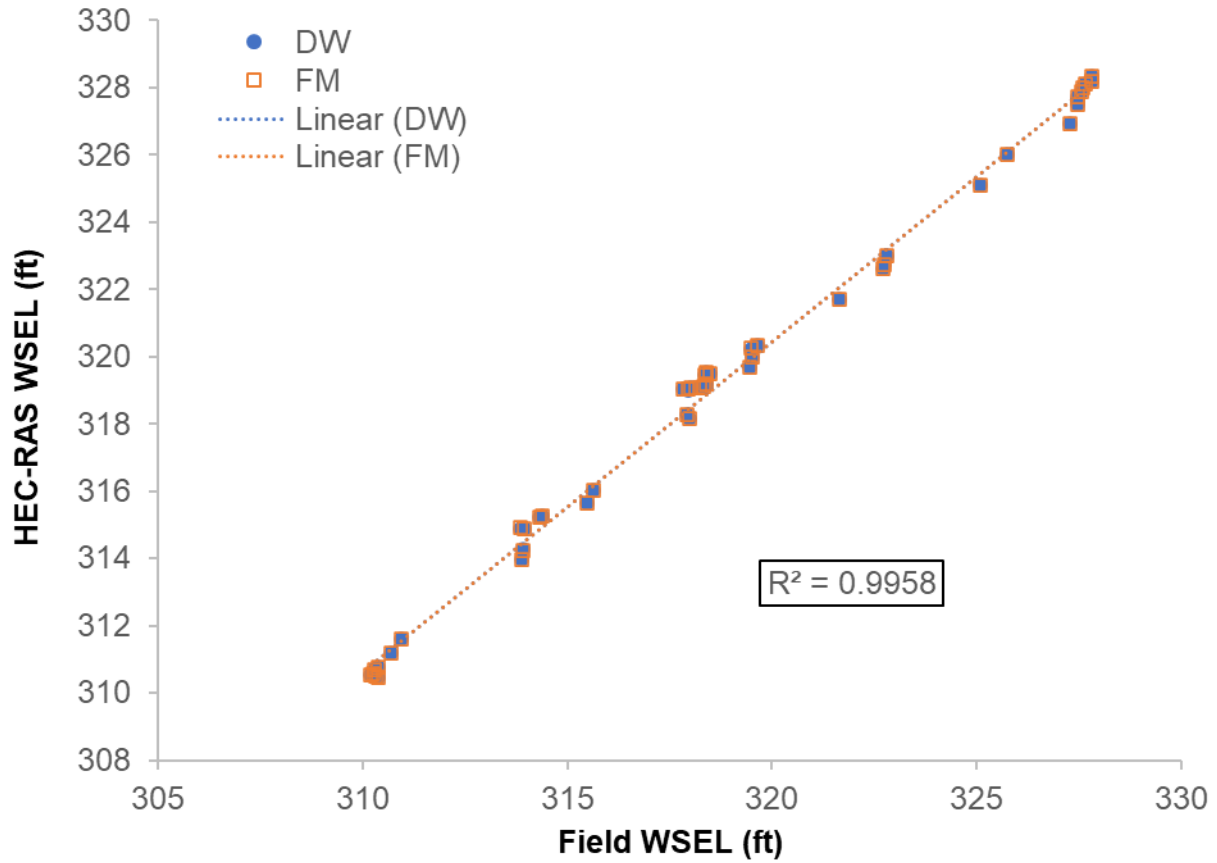


**Figure C-16.** Plot of WSELs derived from bed elevations and depths recorded at each validation depth point with the corresponding WSELs predicted by the model simulation at 17 cfs using the DWA and FM solutions. The  $R^2$  for the DWA solution and FM solution were equal to 0.9958.

## APPENDIX D: PRE-STORM CRITICAL RIFFLE RESULTS

Flow simulations for each Pre-storm model transect (see Table 5 in the main report).

**Table D-1. R23-1.**

Flow (cfs)	Wetted Width (ft)	Total Width (ft)	Contiguous Width (ft)	Percent Total Width	Percent Contiguous Width
50	18.0	0.0	0.0	0%	0%
100	39.0	4.0	4.0	4%	4%
150	75.0	7.5	7.5	8%	8%
200	85.0	13.5	10.0	14%	10%
250	97.0	19.5	12.0	20%	12%

**Table D-2. R23-2.**

Flow (cfs)	Wetted Width (ft)	Total Width (ft)	Contiguous Width (ft)	Percent Total Width	Percent Contiguous Width
50	26.5	0.0	0.0	0%	0%
100	51.5	0.0	0.0	0%	0%
150	88.5	5.0	5.0	5%	5%
200	102.5	9.5	9.5	9%	9%
250	105.0	14.0	11.5	13%	11%

**Table D-3. R23-3.**

Flow (cfs)	Wetted Width (ft)	Total Width (ft)	Contiguous Width (ft)	Percent Total Width	Percent Contiguous Width
50	32.5	0.0	0.0	0%	0%
100	75.0	3.0	3.0	3%	3%
150	83.5	9.0	7.0	10%	8%
200	88.5	17.0	10.5	19%	12%
250	105.0	27.0	14.5	26%	14%

**Table D-4. R23-4.**

Flow (cfs)	Wetted Width (ft)	Total Width (ft)	Contiguous Width (ft)	Percent Total Width	Percent Contiguous Width
50	46.5	0.0	0.0	0%	0%
100	78.0	8.5	8.5	8%	8%
150	91.0	15.0	12.5	13%	11%
200	108.5	21.5	16.0	19%	14%
250	111.5	26.0	19.5	23%	17%

**Table D-5. R23-5.**

Flow (cfs)	Wetted Width (ft)	Total Width (ft)	Contiguous Width (ft)	Percent Total Width	Percent Contiguous Width
50	139.0	8.0	8.0	4%	4%
100	168.0	20.0	11.0	11%	6%
150	175.5	31.5	13.0	17%	7%
200	184.0	40.5	14.5	22%	8%
250	184.0	49.5	15.5	27%	8%

**Table D-6. R23-6.**

Flow (cfs)	Wetted Width (ft)	Total Width (ft)	Contiguous Width (ft)	Percent Total Width	Percent Contiguous Width
50	125.0	17.0	10.5	10%	6%
100	160.0	30.5	20.0	18%	11%
150	168.5	45.5	22.5	26%	13%
200	174.0	75.0	24.5	43%	14%

**Table D-7. R22-1.**

Flow (cfs)	Wetted Width (ft)	Total Width (ft)	Contiguous Width (ft)	Percent Total Width	Percent Contiguous Width
50	14.5	0.0	0.0	0%	0%
100	18.5	7.0	7.0	23%	23%
150	26.5	6.0	6.0	20%	20%
200	28.0	10.0	10.0	33%	33%
250	30.0	16.5	16.5	55%	55%

**Table D-8. R22-2.**

Flow (cfs)	Wetted Width (ft)	Total Width (ft)	Contiguous Width (ft)	Percent Total Width	Percent Contiguous Width
50	15.5	0.0	0.0	0%	0%
100	20.5	0.0	0.0	0%	0%
150	29.0	0.0	0.0	0%	0%
200	31.5	4.5	4.5	13%	13%
250	33.0	14.5	14.5	42%	42%
300	34.5	17.5	17.5	51%	51%

**Table D-9. R22-3.**

Flow (cfs)	Wetted Width (ft)	Total Width (ft)	Contiguous Width (ft)	Percent Total Width	Percent Contiguous Width
50	17.0	0.0	0.0	0%	0%
100	24.0	0.0	0.0	0%	0%
150	28.5	8.0	8.0	22%	22%
200	31.0	12.0	12.0	33%	33%
250	36.0	16.0	16.0	44%	44%

**Table D-10. R20-1.**

Flow (cfs)	Wetted Width (ft)	Total Width (ft)	Contiguous Width (ft)	Percent Total Width	Percent Contiguous Width
50	60.0	2.5	2.5	2%	2%
100	70.0	9.5	5.0	9%	5%
150	99.5	12.0	7.0	11%	7%
200	102.0	13.5	8.0	13%	8%
300	105.0	18.0	10.0	17%	10%

**Table D-11. R20-2.**

Flow (cfs)	Wetted Width (ft)	Total Width (ft)	Contiguous Width (ft)	Percent Total Width	Percent Contiguous Width
50	63.5	0.0	0.0	0%	0%
100	79.0	0.0	0.0	0%	0%
150	103.0	6.5	4.0	6%	4%
200	107.5	14.5	8.5	13%	8%
250	109.5	24.0	10.0	22%	9%
300	111.0	33.5	11.5	30%	10%

**Table D-12. R20-3.**

Flow (cfs)	Wetted Width (ft)	Total Width (ft)	Contiguous Width (ft)	Percent Total Width	Percent Contiguous Width
50	58.0	0.0	0.0	0%	0%
100	72.0	0.0	0.0	0%	0%
150	106.0	4.0	2.5	3%	2%
200	108.5	9.5	5.5	8%	5%
300	113.0	26.5	9.0	23%	8%
400	115.0	38.0	11.0	33%	10%

**Table D-13. R20-4.**

Flow (cfs)	Wetted Width (ft)	Total Width (ft)	Contiguous Width (ft)	Percent Total Width	Percent Contiguous Width
50	61.5	0.0	0.0	0%	0%
100	82.5	7.5	4.0	7%	4%
150	98.0	14.0	6.0	13%	6%
200	102.5	23.5	9.5	22%	9%
250	106.0	36.5	17.5	34%	17%

**Table D-14. R20-5.**

Flow (cfs)	Wetted Width (ft)	Total Width (ft)	Contiguous Width (ft)	Percent Total Width	Percent Contiguous Width
50	60.0	4.0	2.0	4%	2%
100	92.0	18.5	11.5	18%	11%
150	100.0	24.0	14.5	23%	14%
200	102.5	29.0	16.5	28%	16%

**Table D-15. R20-6.**

Flow (cfs)	Wetted Width (ft)	Total Width (ft)	Contiguous Width (ft)	Percent Total Width	Percent Contiguous Width
50	66.0	8.0	5.5	8%	5%
100	91.5	16.5	11.0	16%	11%
150	100.5	22.0	13.0	21%	13%
200	103.5	27.0	14.5	26%	14%

**Table D-16. R20-7.**

Flow (cfs)	Wetted Width (ft)	Total Width (ft)	Contiguous Width (ft)	Percent Total Width	Percent Contiguous Width
50	60.5	9.0	5.0	9%	5%
100	85.0	18.0	10.5	19%	11%
150	90.0	27.5	14.0	28%	14%
200	97.0	41.0	32.5	42%	34%

**Table D-17. R18-1.**

Flow (cfs)	Wetted Width (ft)	Total Width (ft)	Contiguous Width (ft)	Percent Total Width	Percent Contiguous Width
50	29.5	6.5	6.5	19%	19%
100	31.5	8.5	8.5	25%	25%
150	32.0	11.5	10.5	34%	31%
200	33.5	14.0	12.5	42%	37%

**Table D-18. R18-2.**

Flow (cfs)	Wetted Width (ft)	Total Width (ft)	Contiguous Width (ft)	Percent Total Width	Percent Contiguous Width
50	31.0	3.5	3.0	8%	7%
100	33.5	9.0	5.5	20%	12%
150	35.0	14.0	9.5	30%	21%
200	46.0	18.5	13.5	40%	29%

**Table D-19. R18-3.**

Flow (cfs)	Wetted Width (ft)	Total Width (ft)	Contiguous Width (ft)	Percent Total Width	Percent Contiguous Width
50	30.0	2.5	2.5	3%	3%
100	41.5	4.5	4.5	6%	6%
150	60.5	5.0	5.0	6%	6%
200	64.5	6.0	6.0	8%	8%
300	73.5	10.0	8.0	13%	10%
400	78.0	29.5	13.0	38%	17%

**Table D-20. R14-1.**

<b>Flow (cfs)</b>	<b>Wetted Width (ft)</b>	<b>Total Width (ft)</b>	<b>Contiguous Width (ft)</b>	<b>Percent Total Width</b>	<b>Percent Contiguous Width</b>
50	15.5	1.5	1.5	3%	3%
100	39.0	2.0	2.0	4%	4%
150	47.0	10.5	4.0	19%	7%
200	54.5	14.0	10.0	26%	18%

**Table D-21. R11-1.**

<b>Flow (cfs)</b>	<b>Wetted Width (ft)</b>	<b>Total Width (ft)</b>	<b>Contiguous Width (ft)</b>	<b>Percent Total Width</b>	<b>Percent Contiguous Width</b>
50	21.0	0.0	0.0	0%	0%
100	30.0	0.0	0.0	0%	0%
150	38.0	7.0	5.0	15%	11%
200	43.0	23.5	16.5	51%	36%
250	46.0	28.0	28.0	61%	61%

**Table D-22. CS4-CRA.**

<b>Flow (cfs)</b>	<b>Wetted Width (ft)</b>	<b>Total Width (ft)</b>	<b>Contiguous Width (ft)</b>	<b>Percent Total Width</b>	<b>Percent Contiguous Width</b>
50	40.5	3.0	1.5	4%	2%
100	56.0	20.5	7.0	25%	8%
150	75.0	27.5	9.0	33%	11%
200	83.2	34.0	10.0	41%	12%

## APPENDIX E: POST-STORM CRITICAL RIFFLE RESULTS

Flow simulations for each Post-storm model transect (see Table 11 in the main report).

**Table E-1. R23-3.**

Flow (cfs)	Wetted Width (ft)	Total Width (ft)	Contiguous Width (ft)	Percent Total Width	Percent Contiguous Width
50	80.5	15.1	11.5	15%	12%
100	88.2	19.6	16.5	20%	17%
150	91.1	32.1	17.3	32%	18%
200	93.6	37.6	17.3	38%	18%
300	96.2	47.4	17.8	48%	18%
400	98.9	57.3	25.2	58%	25%

**Table E-2. R23-B.**

Flow (cfs)	Wetted Width (ft)	Total Width (ft)	Contiguous Width (ft)	Percent Total Width	Percent Contiguous Width
50	82.4	7.2	4.3	6%	4%
100	91.6	21.5	5.9	19%	5%
125	94.8	25.7	8.8	23%	8%
130	95.2	27.4	9.9	24%	9%
135	95.7	29.2	10.1	26%	9%
150	98.5	33.8	10.3	30%	9%
200	99.3	42.9	18.7	38%	17%
300	108.1	57.4	21.9	51%	20%
400	112.1	66.4	44.2	59%	39%

**Table E-3. R23-C.**

Flow (cfs)	Wetted Width (ft)	Total Width (ft)	Contiguous Width (ft)	Percent Total Width	Percent Contiguous Width
50	84.3	13.1	4.8	11%	4%
100	94.7	27.1	5.8	23%	5%
120	100.1	34.2	9.9	30%	9%
125	100.5	35.8	9.9	31%	9%
130	101.5	36.2	9.9	31%	9%
140	103.7	39.6	11.0	34%	10%
150	104.7	44.9	11.6	39%	10%
200	108.7	55.6	16.3	48%	14%
300	113.0	68.5	23.2	59%	20%
400	115.4	76.5	24.4	66%	21%

**Table E-4. R23-D.**

Flow (cfs)	Wetted Width (ft)	Total Width (ft)	Contiguous Width (ft)	Percent Total Width	Percent Contiguous Width
50	93.3	15.4	5.8	13%	5%
100	99.4	33.0	11.4	28%	10%
150	105.1	45.4	15.1	39%	13%
200	110.0	54.7	16.2	47%	14%
300	113.9	71.2	43.5	61%	37%
400	117.1	76.0	44.6	65%	38%

**Table E-5. R23-E.**

Flow (cfs)	Wetted Width (ft)	Total Width (ft)	Contiguous Width (ft)	Percent Total Width	Percent Contiguous Width
50	143.2	23.8	5.8	14%	3%
100	162.4	42.4	8.9	24%	5%
150	170.8	69.1	21.3	39%	12%
200	173.9	80.4	36.5	46%	21%
300	175.5	98.7	47.1	56%	27%
400	175.5	108.7	47.6	62%	27%

**Table E-6. R23-F.**

Flow (cfs)	Wetted Width (ft)	Total Width (ft)	Contiguous Width (ft)	Percent Total Width	Percent Contiguous Width
50	150.6	23.7	7.1	14%	4%
100	159.0	49.1	10.3	29%	6%
150	163.8	88.9	32.8	52%	19%
200	164.2	98.5	39.0	58%	23%
300	167.9	122.1	73.8	71%	43%
400	171.2	133.7	74.6	78%	44%

**Table E-7. R20-A.**

Flow (cfs)	Wetted Width (ft)	Total Width (ft)	Contiguous Width (ft)	Percent Total Width	Percent Contiguous Width
50	99.6	25.0	7.1	22%	6%
100	107.0	37.3	10.5	32%	9%
150	110.4	57.6	24.3	50%	21%
200	112.9	73.4	33.0	64%	29%
300	114.1	92.2	36.7	80%	32%
400	115.2	98.2	58.5	85%	51%

**Table E-8. R20-B.**

Flow (cfs)	Wetted Width (ft)	Total Width (ft)	Contiguous Width (ft)	Percent Total Width	Percent Contiguous Width
50	93.4	17.2	6.0	16%	5%
100	98.2	29.9	7.2	27%	7%
150	102.2	45.0	15.0	41%	14%
200	105.7	58.7	15.0	53%	14%
300	108.9	80.1	15.7	73%	14%
400	109.8	90.0	27.6	82%	25%

**Table E-9. R20-C.**

Flow (cfs)	Wetted Width (ft)	Total Width (ft)	Contiguous Width (ft)	Percent Total Width	Percent Contiguous Width
50	98.6	17.4	4.8	15%	4%
100	107.1	40.2	8.3	35%	7%
125	110.3	51.0	9.6	44%	8%
130	110.9	56.8	10.3	49%	9%
150	112.9	61.6	11.5	53%	10%
200	113.5	71.6	13.3	62%	12%
300	114.8	90.0	34.6	78%	30%
400	115.3	95.2	40.9	83%	36%

**Table E-10. R20-D.**

Flow (cfs)	Wetted Width (ft)	Total Width (ft)	Contiguous Width (ft)	Percent Total Width	Percent Contiguous Width
50	99.9	18.6	7.0	17%	6%
100	105.6	43.6	9.6	40%	9%
150	107.5	70.7	22.2	65%	20%
200	108.2	80.6	23.9	74%	22%
300	108.5	91.8	41.3	84%	38%
400	109.4	98.4	50.2	90%	46%

**Table E-11. R20-E.**

Flow (cfs)	Wetted Width (ft)	Total Width (ft)	Contiguous Width (ft)	Percent Total Width	Percent Contiguous Width
50	91.7	36.1	11.6	35%	11%
100	98.5	60.9	14.7	59%	14%
150	99.7	73.9	42.7	72%	42%
200	99.7	80.0	44.2	78%	43%
300	102.5	85.9	44.4	84%	43%
400	102.8	89.6	45.2	87%	44%

**Table E-12. R16-CRA.**

Flow (cfs)	Wetted Width (ft)	Total Width (ft)	Contiguous Width (ft)	Percent Total Width	Percent Contiguous Width
50	25.5	8.4	2.5	22%	7%
100	29.0	14.9	13.9	39%	36%
150	31.6	17.7	17.7	46%	46%
200	33.5	18.6	18.1	48%	47%
300	38.0	21.4	19.1	55%	50%
400	38.5	23.3	20.0	60%	52%

**Table E-13. R12-CRA.**

Flow (cfs)	Wetted Width (ft)	Total Width (ft)	Contiguous Width (ft)	Percent Total Width	Percent Contiguous Width
50	44.4	5.5	2.3	9%	4%
100	48.2	24.2	10.8	38%	17%
150	50.5	33.8	17.3	53%	27%
200	54.3	36.6	18.0	57%	28%
300	61.3	44.6	21.6	70%	34%
400	63.8	46.1	22.2	72%	35%

**Table E-14. R8-CRA.**

Flow (cfs)	Wetted Width (ft)	Total Width (ft)	Contiguous Width (ft)	Percent Total Width	Percent Contiguous Width
50	81.1	0.2	0.2	0%	0%
100	84.9	10.2	2.6	11%	3%
105	87.0	26.9	6.5	29%	7%
140	89.1	35.8	7.5	39%	8%
145	89.1	36.9	10.4	40%	11%
150	89.1	38.1	10.4	41%	11%
200	89.9	47.7	12.6	52%	14%
300	91.9	58.9	13.9	64%	15%
400	92.5	64.4	24.7	70%	27%

**Table E-15. R2-CRA.**

<b>Flow (cfs)</b>	<b>Wetted Width (ft)</b>	<b>Total Width (ft)</b>	<b>Contiguous Width (ft)</b>	<b>Percent Total Width</b>	<b>Percent Contiguous Width</b>
50	50.8	10.6	5.6	18%	9%
100	56.5	31.3	13.8	52%	23%
150	58.1	46.2	31.2	77%	52%
200	59.4	52.3	35.2	87%	58%
300	59.7	55.6	36.8	92%	61%
400	60.3	57.1	37.9	95%	63%

**APPENDIX F: VENTURA COUNTY SURVEY FIELD NOTES  
FOR POINT NUMBER 1104**

FIELD SURVEY NOTES  
TITLE SHEET

Project: <u>Santa Ana Boulevard Bridge Improvements</u>		Project No: <u>81919</u>
		Date Began Survey: <u>01/29/20</u>
		Date Completed: <u>01/29/20</u>
Project Log No: <u>2020-005</u>		Chief of Party: <u>K. Farokhi</u>
		Field Survey No: <u>2020-005</u>
Location of Survey: _____ <u>Southwest of Santa Ana Boulevard &amp; Bridge</u>		
Type of Survey: <u>Topography</u>		
Survey Description and Purpose: <u>Perform Survey to locate Sewer Pipe, for design purposes</u>		
Reference Material: <u>VCFB 2012-023</u>		
		Party Personnel:
		<u>K. Farokhi</u>
		<u>M. Vasquez</u>
Horizontal Datum: <u>CCS83, Zone 5, 2004.00 Epoch (US Feet)</u>		
Vertical Datum: <u>NAVD 88, Ven. Co. Pub. 1992 (US Feet)</u>		
Instruments: <u>Trimble S7 Total Station, S/N 37210293</u>		
Notes Reviewed By: 	Date: <u>3/31/2020</u>	
Additional Information: _____		

Figure F-1. County of Ventura field survey notes title sheet.

### SURVEY NOTES

PROJECT: Santa Ana Boulevard Bridge Improvement

CHIEF OF PARTY: K. Farokhi      DATE: Jan. 2020

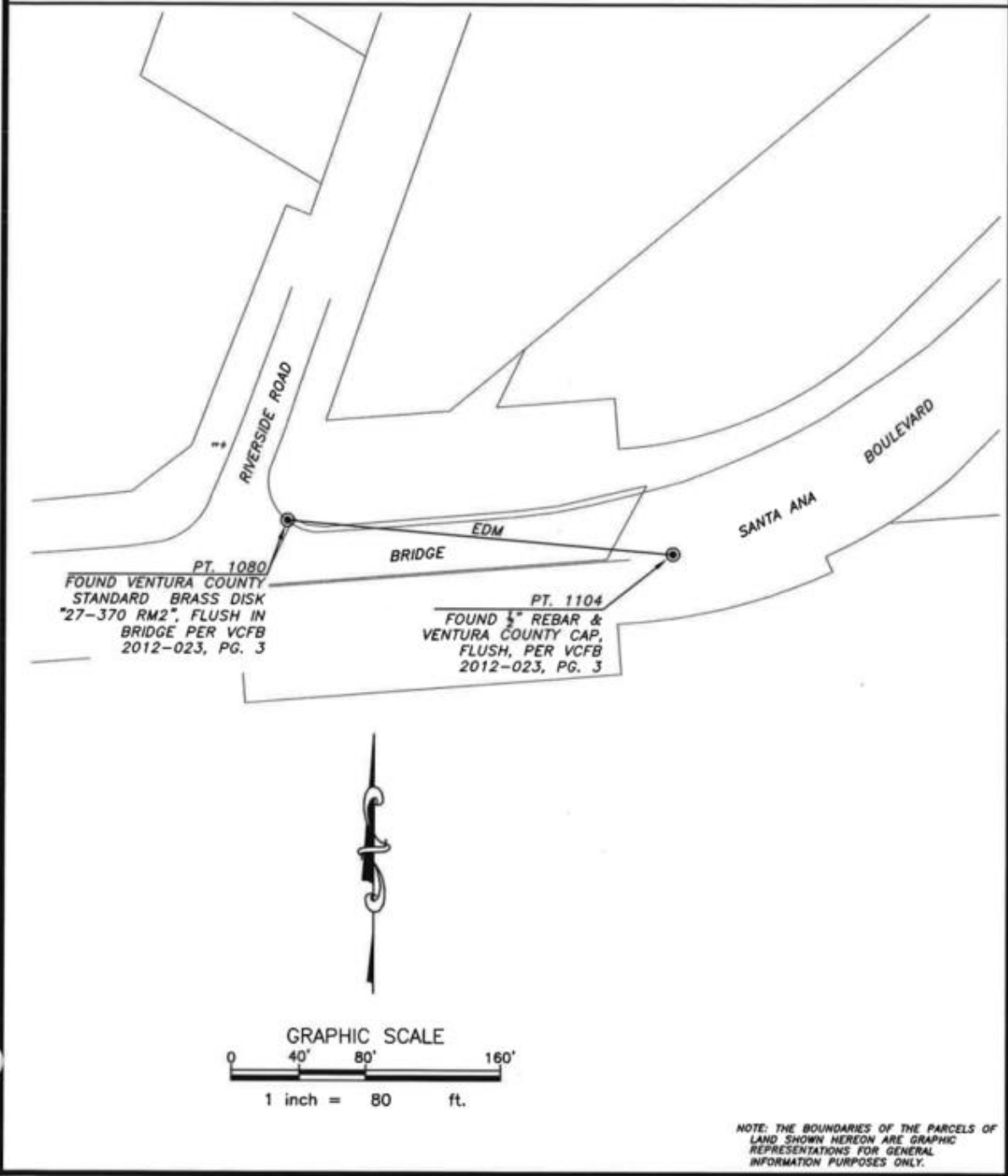


Figure F-2. County of Ventura survey map.

ADJUSTED COORDINATES

Horizontal Datum: NAD83, CCS Zone 5, 2004.00 Epoch, (US Feet)

Vertical Datum: NAVD 88, Ven. Co. Pub. 1992 (US Feet)

POINT	NORTHING	EASTING	Elev.	Description
1080*	1970393.93	6166938.61	412.25	BM: 27-370 RM2
1104*	1970374.03	6167168.73	412.88	1/2" Rebar

\*= Coordinates held per VCFB 2012-023, pg. 4

Figure F-3. County of Ventura survey coordinates.

## REFERENCES

- Airborne 1 (2005). LiDAR mapping report v1.2. Available: <https://map.dfg.ca.gov/metadata/ds0518.html>.
- CDFW (2018). Draft instream flow criteria Mill Creek, Tehama County. California Department of Fish and Wildlife, Water Branch, Instream Flow Program (CDFW), Sacramento, CA.
- Chow, V. T. (1959). In Open-channel hydraulics. McGraw-Hill, New York. pp. 680.
- CMWD (2010). 2010 Robles Fish Passage Facility progress report. Casitas Municipal Water District (CMWD), Oak View, CA.
- Cowan, W. R., D. E. Rankin and M. Gard (2016). Evaluation of Central Valley spring-run Chinook Salmon passage through Lower Butte Creek using hydraulic modelling techniques. *River Research and Applications* **33**(3): 328-340.
- ESRI (2011). ArcGIS Desktop: Release 10. Redlands, CA, Environmental Systems Research Institute (ESRI).
- Ghanem, A., P. Steffler, F. Hicks and C. Katopodis (1996). Two-dimensional hydraulic simulation of physical habitat conditions in flowing streams. *Regulated Rivers: Research and Management* **12**: 185-200.
- Gupta, R. S. (1995). Hydrology and hydraulic systems. Waveland Press, Inc, Prospect Heights, IL.
- HEC-RAS (2018). Version 5.0.6 [computer software]. Davis, CA, U.S. Army Corps of Engineers, Hydraulic Engineering Center.
- Holmes, R. W., D. E. Rankin, E. Ballard and M. Gard (2016). Evaluation of steelhead passage flows using hydraulic modeling on an unregulated coastal California river. *River Research and Applications* **32**: 697-710.
- Lewis, S. D. and M. W. Gibson (2009). 2009 monitoring and evaluation study plan for the Robles Fish Passage Facility and related studies, Casitas Municipal Water District, Oak View, CA.

Munson, B. R., D. F. Young and T. H. Okiishi (1998). Fundamentals of fluid mechanics. 3rd edition. John Wiley & Sons Inc.

NOAA (2020a). National geodetic survey data explorer. National Oceanic and Atmospheric Administration, National Geodetic Survey (NOAA). Available: <https://www.ngs.noaa.gov/NGSDDataExplorer/>. Accessed: 09/22/2020.

NOAA (2020b). Online vertical datum transformation. National Oceanic and Atmospheric Administration, NOAA. Available: <https://vdatum.noaa.gov/vdatumweb/vdatumweb?a=172103320190523>. Accessed: 09/22/2020.

NOAA (2020c). OPUS: Online positioning user service. National Oceanic and Atmospheric Administration, National Geodetic Survey (NOAA). Available: <https://www.ngs.noaa.gov/OPUS/>. Accessed: 02/21/2020.

Steffler, P. (2002). R2D\_Bed: Bed topography file editor. User's manual. University of Alberta, Edmonton, Alberta.

Steffler, P. and J. Blackburn (2002). River 2D: Two-dimensional depth average model of river hydrodynamics and fish habitat. Introduction to depth averaged modeling and user's manual. University of Alberta, Edmonton, Alberta.

Towill Inc (2018). Ventura AOI LiDAR. Prepared for the State of California Department of General Services, Emergency Resource Support and Logistics Management, West Sacramento, CA.

USACE (2016). HEC-RAS river analysis system. Hydraulic reference manual. Version 5.0. U.S. Army Core of Engineers, Hydrologic Engineering Center (USACE), Davis, CA. Available: <https://www.hec.usace.army.mil/software/hecras/documentation/HEC-RAS%205.0%20Reference%20Manual.pdf>.

USFWS (2011). Sacramento Fish and Wildlife office standards for Physical Habitat Simulation studies. U.S. Fish and Wildlife Service, Sacramento Fish and Wildlife Office, Restoration and Monitoring Program (USFWS), Sacramento, CA.

USGS (2001). PHABSIM for Windows, user's manual and exercises. U.S. Geological Survey, Midcontinent Ecological Science Center (USGS), Fort Collins, CO. Open File Report 01-340.

USGS (2018). Lidar base specification. In Chapter 4 of Section B, U.S. Geological Survey standards. Book 11, collection and deliniation of spatial data. H. K. Heidemann (editor). U.S. Geological Survey, National Geospatial Program (USGS), Reston, VA. Available: <https://pubs.usgs.gov/tm/11b4/pdf/tm11-B4.pdf>.

Waddle, T. and P. Steffler (2002). Mesh generation program for River2D two dimensional depth averaged finite element, introduction to mesh generation and user's manual. University of Alberta, Edmonton, Alberta.

WEST Consultants Inc (2017). Two-dimensional modeling using HEC-RAS. HEC-RAS 5.0 Workshop.

Yalin, M. S. (1977). Mechanics of sediment transport. 2nd edition. Pergamon Press, Ontario, Canada.